

DIFFUSERS IN COHERENTLY ILLUMINATED, WIDE FIELD OF VIEW APPLICATIONS

by

Garret Odom

Copyright © Garret Odom 2016

A Thesis Submitted to the Faculty of the

COLLEGE OF OPTICAL SCIENCES

In Partial Fulfillment of the Requirements

For the Degree of

MASTER OF SCIENCE

In the Graduate College

THE UNIVERSITY OF ARIZONA

2016

STATEMENT BY AUTHOR

The thesis titled *Diffusers in Coherently Illuminated, Wide Field of View Applications* prepared by *Garret Odom* has been submitted in partial fulfillment of requirements for a master's degree at the University of Arizona and is deposited in the University Library to be made available to borrowers under rules of the Library.

Brief quotations from this thesis are allowable without special permission, provided that an accurate acknowledgement of the source is made. Requests for permission for extended quotation from or reproduction of this manuscript in whole or in part may be granted by the copyright holder.

SIGNED: *Garret Odom*

APPROVAL BY THESIS DIRECTOR

This thesis has been approved on the date shown below:

Yuzuru Takashima
Associate Professor of Optical Sciences

5/12/2016
Date

ACKNOWLEDGEMENTS

I would like to recognize all of the people who have had a part in making my time as a graduate student a success. First, I would like to thank my wife, Jaime, for being my greatest friend and motivator throughout my college career. I also want to thank my family for always providing support and encouragement in all of my endeavors and for challenging me to take on new opportunities.

Special thanks to the faculty and staff of the College of Optical Sciences for making my graduate and undergraduate experiences very enjoyable. Thanks to the members of the Takashima Research Group for providing useful dialogue and for your enthusiasm for optics. I would like to recognize Chris Summitt and Sunghin Wang for their assistance in fabricating and measuring my samples. Recognition also goes to Phat Lu for taking time to help me measure the surface profiles of various components.

I would like to acknowledge my employer, Raytheon Missile Systems, for encouraging its employees to pursue higher education. Several of my coworkers were great resources throughout this project and I feel very fortunate to be able to learn from them: Dr. Byron Taylor, Dr. Ron Roncone, and Dr. Mike Schaub. Thanks to each for providing valuable insight, advice, and guidance.

Lastly, I would like to thank the members of my committee for their contributions to my research and for sacrificing their time to help me succeed. My advisor, Yuzuru Takashima, for fostering a conducive research environment and for being very accommodating to my school-work schedule. Tom Milster, for his assistance with Optiscan and for sparking my initial interest in diffractive optics during my time as an undergraduate student. Eric Fest, for initially suggesting this research topic and for helping me navigate my way to the finish line.

TABLE OF CONTENTS

LIST OF FIGURES	6
LIST OF TABLES	8
ABSTRACT.....	9
Chapter 1: Introduction to Diffusers	10
1.1 What is a Diffuser?.....	10
1.2 Ground Glass Diffusers	11
1.3 Bulk/Volume Diffusers	12
1.4 Micro-Prism Diffusers.....	13
1.4.1 Diffractive Prismatic Diffusers.....	14
1.5 Holographic Diffusers	15
1.6 Light Shaping Diffusers	16
1.7 Lenslet Arrays	18
1.8 Engineered Diffusers.....	21
1.9 Diffuser Summary	26
Chapter 2: Diffusers in Laser Spot Trackers	27
2.1 Diffusers and Lenses	27
2.2 Laser Spot Trackers.....	28
2.3 Diffusers in Laser Spot Trackers.....	31
2.4 Diffractive Diffusers in Laser Spot Trackers	34
Chapter 3: Diffractive Diffuser Design.....	35
3.1 Computer Generated Holograms.....	35
3.2 Gerchberg-Saxton Algorithm	36
3.3 Design of a Diffractive Diffuser.....	38
3.4 Limitations of Design.....	41
Chapter 4: Diffractive Diffuser Fabrication, Testing, and System Performance	42
4.1 CGH Fabrication Process	42
4.2 CGH Testing Setup	42
4.3 Off-Axis Behavior of Diffractive Diffusers	43

4.4 Spatial Transfer Function Performance.....	48
Chapter 5: Conclusion.....	49
5.1 So Which Diffuser is the Best?	49
APPENDIX A: The Speckle Phenomenon.....	51
REFERENCES.....	53

LIST OF FIGURES

FIGURE	TITLE	PAGE
Figure 1.1	Surface of a standard ground glass diffuser viewed under 40X magnification.	12
Figure 1.2	Scattering in a bulk diffuser.	13
Figure 1.3	Pyramid type micro-prism array.	14
Figure 1.4	Planar sawtooth type micro-prism array.	14
Figure 1.5	Possible Recording Geometry for Holographic Diffuser.	16
Figure 1.6	40X Magnified Surfaces of a 5° Circular LSD and 60° Circular LSD.	18
Figure 1.7	Lenslet array in a typical wavefront sensor.	19
Figure 1.8	Lenslet array in a diffuser configuration.	20
Figure 1.9	Various packing geometries of a lenslet array.	21
Figure 1.10	10X and 40X magnified surface of a 20° circular Engineered Diffuser.	23
Figure 1.11	Measured intensity as a function of AOI for EDC20 RPC Diffuser.	24
Figure 1.12	Simulated RPC EDC20 lenslet performance for 0°, 15°, and 30° AOI	25
Figure 2.1	Diffuser used without lens.	27
Figure 2.2	Diffuser used with lens.	28
Figure 2.3	Laser Spot Tracker Geometry.	30
Figure 2.4	Focused laser spot on a quad-cell detector.	30
Figure 2.5	Diffuser added to Laser Spot Tracker System.	32
Figure 2.6	Ideal Laser Spot Tracker diffuser performance.	33
Figure 2.7	Actual Performance of RPC EDC 20 at AOI = 0°, 15°, and 30°.	33
Figure 3.1	Basic operation of a CGH.	36
Figure 3.2	The Gerchberg-Saxton algorithm.	37
Figure 3.3	Parameters used in Optiscan to design the CGH.	39
Figure 3.4	SNR of CGH pattern vs iteration number.	39
Figure 3.5	Input image and simulated far field pattern produced by CGH.	40
Figure 3.6	CGH pattern produced by Optiscan.	40
Figure 4.1	Secondary CGH testing configuration.	43

Figure 4.2	Off-Axis illumination of diffractive structure.	44
Figure 4.3	First diffracted orders from a periodic grating	45
Figure 4.4	Diffraction angle vs AOI.	46
Figure 4.5	Angular separation of the +1 and -1 diffraction orders vs AOI.	46
Figure 4.6	Diffused diffraction pattern stretches as the AOI increases.	47
Figure 4.7	Relative spot diameter in x-dimension vs AOI.	47
Figure 4.8	Elevation STF vs AOI for various diffuser types	48
Figure A.1	Wavelets produced by a rough surface.	51
Figure A.2	Speckle pattern produced by a randomly rough surface illuminated by a laser.	52

LIST OF TABLES

TABLE	TITLE	PAGE
Table 1	Summary of diffusers.	26

ABSTRACT

Diffusers are devices that are designed to spread or scatter light. Many different types of diffusers are readily available in the commercial and scientific industries, but most are designed with a specific application in mind. Thus, when attempting to use a diffuser in an unconventional way, it is important to understand how it will behave in the system it will be used in. One example is a diffuser in a coherently illuminated, wide field of view system such as a laser spot tracker. For some diffusers, coherent illumination and/or off-axis illumination can have a major impact on their diffusing properties, which may or may not be acceptable to system performance. This project evaluates the pros and cons of several types of diffusers in order to identify the most effective solution based on the parameters of a system, using a laser spot tracker as an example. First, three diffusers are down selected from the list based on their refractive and diffractive properties. Next, the candidates are evaluated analytically and/or experimentally to characterize their behavior when illuminated by a collimated laser over a wide range of incident angles. Results suggest that a computer generated diffractive diffuser is the most flexible design option for the described laser spot tracker, but some drawbacks such as diffraction efficiency and maximum diffusion angle do need to be considered. This selection method can be extended to serve as a guide for making the proper diffuser choice in many different applications.

CHAPTER 1

Introduction to Diffusers

1.1. What is a Diffuser?

In the simplest sense, an optical diffuser can be described as an object that spreads or scatters light. The meaning of what a diffuser is can vary depending on who you ask. In the field of light calibration, an integrating sphere may be referred to as a diffuser due to the diffuse reflections that occur inside the white walls of the sphere. In the world of cell phone, TV, or computer screens a diffuser is one of the elements placed in front of the illumination source to distribute the light across the screen. Similarly, in the housing or architectural lighting industry a diffuser is anything that can be used to spread light over an area (such as a large wall) to increase energy efficiency and produce more aesthetically pleasing light conditions.

In commercial optics a diffuser is most commonly a thin film or flat piece of glass with a rough surface that diverges and homogenizes, or smoothly distributes, an incident beam of light into a cone. The most common performance specifications for these devices are their divergence angles, intensity distributions, and the shape of their output beam. Another important parameter is the transmission efficiency of the diffuser, which is defined as the ratio of the energy being diffused into the intended pattern over the total amount of energy incident upon the diffuser. The following sections highlight the properties and characteristics of the most common and popular types of commercial diffusers. This chapter is intended to provide a useful reference for determining which diffuser may be best suited for a particular application, especially if the

application is using a diffuser in an uncommon or unique way, as is the case for laser spot tracking systems, which is the focus of this thesis.

1.2 Ground Glass Diffusers

One of the oldest and most commonly used types of commercial diffusers is the ground glass diffuser. These are produced by surface grinding, sandblasting, or chemical etching one or both sides of a glass plate. These processes result in randomly distributed peaks and valleys on the surface of the glass, as can be seen in Figure 1.1. When a beam of light is incident on the diffuser surface, each ray is refracted in a random direction according to a Gaussian statistical distribution and the overall effect is a Gaussian irradiance profile in the observation plane [1]. The manufacturing process for these diffusers is capable only of controlling the average surface roughness, which determines the spread angle of the light and the transmission efficiency of the element. A rougher surface (higher peaks and lower valleys) will produce a wider diffusion pattern but will have higher transmission losses due to increased backscatter [3].

Ground glass diffusers are a popular option for simple light spreading tasks since they can be cheaply mass produced and their properties are well-understood. They have found uses in many applications such as illumination systems, imaging target generation, and display screens, but they are not ideal in other applications since they are strictly limited to circular Gaussian intensity distributions [1,2].

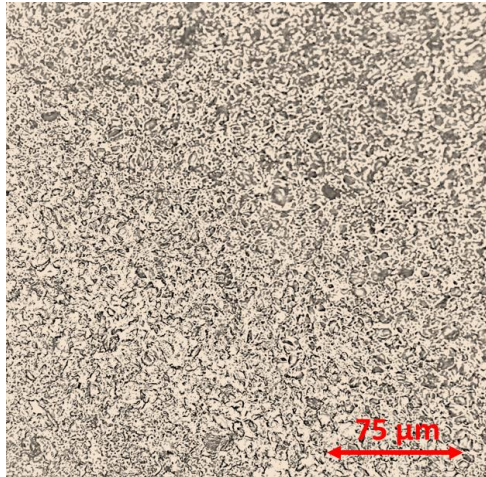


Figure 1.1. Surface of a standard ground glass diffuser viewed under 40X magnification.

1.3 Bulk/Volume Diffusers

Bulk diffusers achieve their diffusion properties through small scattering centers embedded within the volume of the device, which is sometimes called the substrate, host, or matrix. Typical substrate materials include glass, polymethylmethacrylate (PMMA), polycarbonate, or other plastics, while the scattering centers most commonly consist of small glass spheres, plastic particles, or air cavities. The scatter profile of these types of diffusers can be controlled somewhat by adjusting the scatter center size, the thickness of the substrate, and the difference in the refractive index of the two materials. Scatter centers are usually on the order of 5 to 100 μm in diameter, substrate thickness can range from 1 to 10 mm, and refractive index difference is typically around 0.1 [12].

Opal glass is the most common type of bulk diffuser. Light rays traveling through the glass interact with the spherical particles suspended inside and undergo multiple scattering events before emerging from the opposite side (see Figure 1.2). This leads to a nearly Lambertian scatter profile but also results in high amounts of light loss due to backscattering. Typical opal diffusers have only 20-40% transmission efficiency [3]. Many newer plastic diffusers, however, are advertised to have transmission efficiencies exceeding 80% and some

utilize elongated scatter centers in order to achieve elliptical diffusion angles [31]. These properties make bulk diffusers ideal for hiding source structures such as LEDs or light bulbs because the multiple scatter events wash out the spatial details of the structure while transmission efficiency is usually not critical.

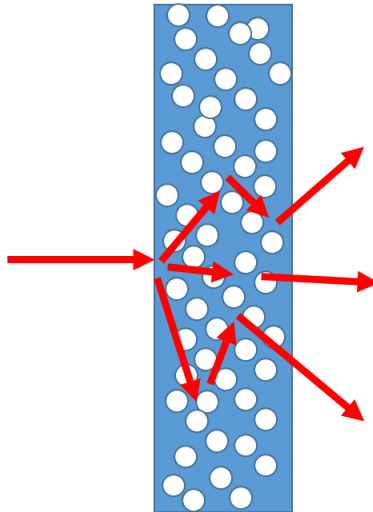


Figure 1.2. Scattering in a bulk diffuser. Scatter centers in bulk diffusers cause rays to undergo multiple scattering events, leading to uniform, but lossy, illumination from the output surface.

1.4 Micro-Prism Diffusers

Micro-prism diffusers are arrays of linear surfaces that form prism-type structures on the front of a substrate typically made of plastic for ease of manufacturing. The prism structures can be 1D or 2D patterns and they can take on forms such as pyramids (Figure 1.3), planar sawtooths (Figure 1.4), circular sawtooths, diamonds, etc. [31-33]. Because of their ability to refract light over broad ranges, these devices are most commonly used in luminaires for large rooms lit by fluorescent tubes or LEDs. As such, the diffusion properties of the micro-prism array will vary widely based on the application and design parameters. The reader is directed to [34] for examples of micro-prism designs and their corresponding light distributions.

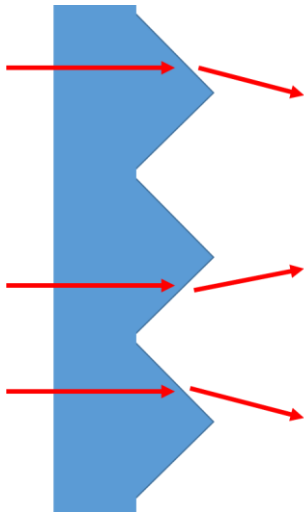


Figure 1.3. Pyramid type array

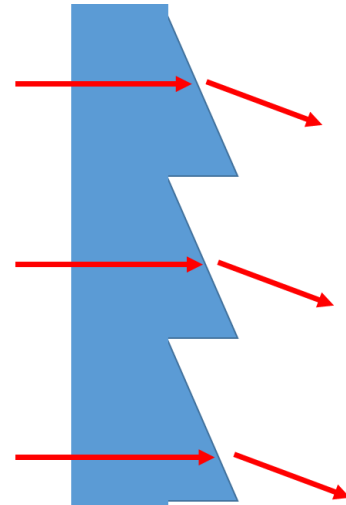


Figure 1.4. Planar sawtooth type array

1.4.1 Diffractive Prismatic Diffusers

The commercial prismatic diffusers described above typically have surface features on the order of 0.5 to 5 mm so they are purely refractive elements, but in some special applications where coherent illumination is used, better diffusion control can be achieved by shrinking the surface features down to the range of 1 μm so the diffuser works in the diffraction regime (which occurs when the feature size of the diffuser is approximately the same size as the wavelength of light). Common diffractive elements with prismatic shapes include the diffractive Fresnel lens and the blazed (sawtooth) diffraction grating. In 1973, Kurtz et al [2] proposed a design method that controls the probability density of the surface slopes distributed across a diffuser in order to achieve a well-defined angular spectrum transmitted through the structure. In other words, each facet of every micro-surface is assigned a slope value according to a pre-defined probability density function which directly translates to an array of spatial frequency components contained upon the diffuser. According to diffraction theory, the spatial frequency components of the diffuser determine the angular spectrum of the diffracted light which means specific control of the diffusion pattern can be achieved, thus the term “band-limited diffuser” was coined to

indicate the ability to control the angular spectrum of the diffused light. This idea was further developed by Mendez et al [35, 36], highlighting the theoretical ability of randomized prismatic facets to produce arbitrary pattern shapes and intensity profiles ranging from Lambertian to tophat rectangular patterns. In practice it seems that fabrication of this type of design is difficult because the faceted surfaces have very sharp, well-defined edges that are difficult fabricate. Even though this product hasn't seen much commercial success, the design concept is useful for being able to understand the diffuser designs discussed in Sections 1.8 and 3.1.

1.5 Holographic Diffusers

A true holographic diffuser is a recording of the interference between a speckle pattern (typically produced by a standard ground glass diffuser) and a reference beam, as depicted in Figure 1.5. This can be done either in a volume recording material or on a recording surface such as a photosensitive polymer. Various geometries are possible with this method and this provides additional capabilities that are not possible with traditional diffusers. For example, Meyerhofer [13] proposed using holographic diffusers in backlit screens because they can provide higher transmission scattering efficiency and unique illumination properties due to the special scattering properties at various angles of incidence. Additionally, Pawluczyk [10] produced holographic diffusers that were optimized for off-axis illumination in display or projection systems to improve the image being seen by an observer at an oblique viewing angle. He goes on to explain that these types of diffusers can achieve more controlled angular scattering distributions that can be tailored for specific applications.

The disadvantages of this type of diffuser include tighter tolerances and more expensive fabrication processes, difficulty producing large components, and susceptibility to a large magnitude zero order (specular) component in the diffused beam. These factors, along with the

fact that such a diffuser is typically specialized for a specific application, are the primary reasons why holographic diffusers are not often commercially available.

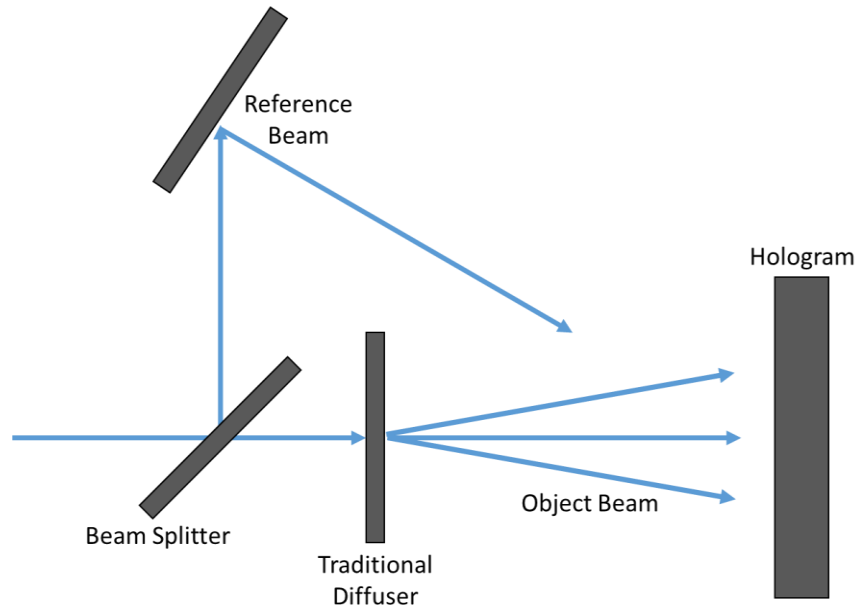


Figure 1.5. Possible Recording Geometry for Holographic Diffuser (Note: Many Other Geometries are Possible)

1.6 Light Shaping Diffusers

A major drawback of the holographic diffusers of Section 1.5 is that the recording geometries often require off-axis illumination when playing back the holographic pattern. This is a problem for many applications where the light source is on-axis with the hologram because it results in lower diffraction efficiency and undesirable effects such as higher zero order. Therefore, it is desirable to have a diffusing element that possesses the well-controlled scattering capabilities of a holographic diffuser without some of the limiting factors described above. The Light Shaping Diffuser (LSD) produced by Luminit, LLC (a spinoff of Physical Optics Corporation) helps solve this problem.

The LSD is produced in a similar fashion to a holographic diffuser except there is no reference beam used in the recording process [4, 5, 11]. A coherent beam illuminates a

traditional diffuser to create a diverging beam of scattered light containing speckle (see Appendix A for more detail). The speckles can be shaped and rearranged via lenses and masking apertures placed prior to the photosensitive medium. The final result is a random exposure pattern that will scatter the light according to the size and shape of the speckles recorded in the medium. This allows the LSD to achieve a wide range of scattering angles, circular or elliptical spatial profiles, and high transmission efficiency. Jansson et al. [4] originally proposed recording the diffuser pattern in a volume holographic material where the speckle recording would result in smooth variations of the refractive index within the medium. This results in higher maximum scatter angle and less backscattered light compared to other volume diffusers such as those discussed in Section 1.3. Several years later, Petersen et al. [5] claimed that a similar effect could be achieved by recording a speckle pattern on the surface of a photoresist material. This results in random variations in the surface height rather than variations in the refractive index, which makes the diffuser easier to mass produce. In this sense, the surface relief version of LSD is very similar to a piece of ground glass except additional scattering capabilities are embedded in the LSD based on the shape and size of the speckles used to record it.

Figure 1.6 shows two different commercial LSDs purchased from Newport [20] viewed under 40X magnification. It is clear to see that the less divergent diffuser has larger surface features while the more divergent diffuser has much smaller surface features corresponding to the smaller speckles used to record it.

One point worth noting is that because the recording process is similar to traditional holography, LSDs are commonly referred to as holographic diffusers [11,20]. Sometimes the term “single beam holography” is used to distinguish between traditional holographic recording (i.e. two beam holography) and LSD recording. As was already discussed, a true hologram

requires interference between an object beam and reference beam. The benefit of the LSD is that it does not require a reconstruction beam like a traditional hologram. This means that, like ground glass diffusers, LSDs can be used with coherent or incoherent light sources to still achieve essentially the same effect [24], making them popular options for applications such as stage lighting, blending light sources, and other homogenization tasks where higher transmission efficiency is desired.

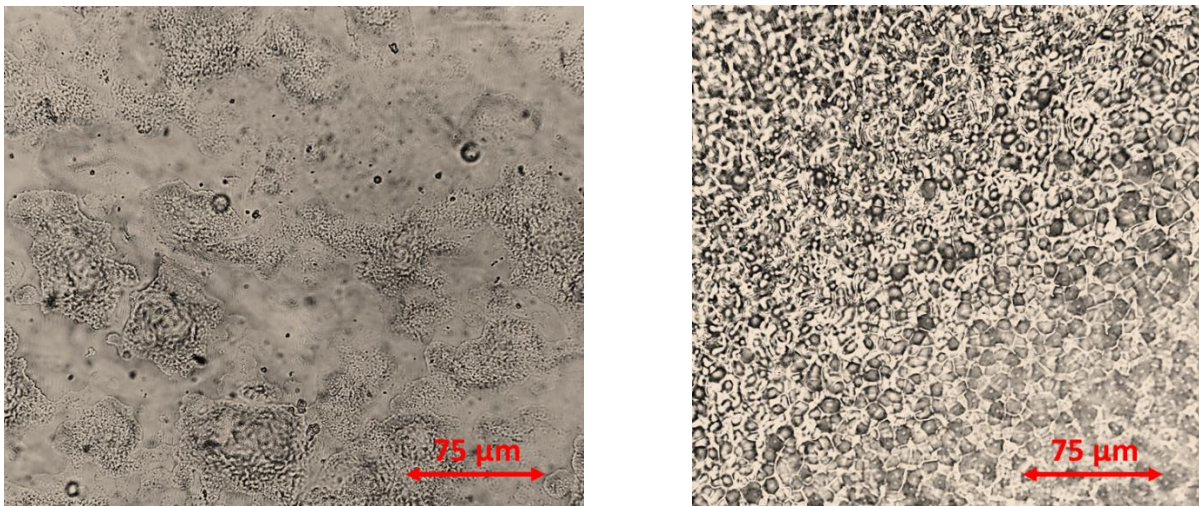


Figure 1.6. 40X Magnified Surfaces of a 5° Circular LSD (left) and 60° Circular LSD (right)

1.7 Lenslet Arrays

A lenslet array, or sometimes called a micro-lens array, is a group of closely spaced lenses with diameters that typically range from about 25 μm to 1 mm [6]. Lenses of this size function the same as a standard lens but the primary difference is in how they are fabricated. Standard lenses are typically ground and polished while micro-lenses are made via laser lithography techniques. A lenslet array is useful because it can sample an incident wavefront and divide it into smaller segments, allowing control of the spatial and/or angular properties of the wavefront. For this reason, lenslet arrays have found their way into many well-known devices such as the Kohler integrator (also known as the fly's eye integrator) [27], the Shack-Hartman

wavefront sensor [28], video projectors, and imaging systems such as the light field camera [29].

Figure 1.7 shows how a lenslet array is used in a wavefront sensor to measure the distortion caused by atmospheric turbulence.

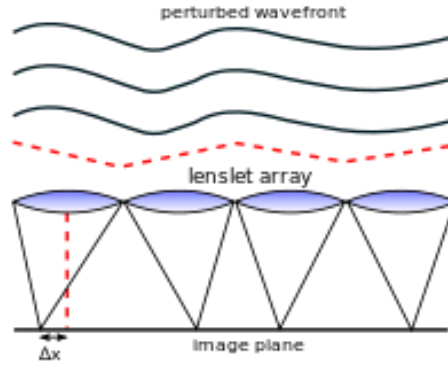


Figure 1.7. Lenslet array in a typical wavefront sensor where the local slope of the wavefront is converted into spatial deviation of a focused point on a detector element (image courtesy wikipedia.org/wiki/Shack-Hartmann_wavefront_sensor).

Lenslet arrays can also be used as beam homogenizers, beam shapers, and diffusers for illumination applications. Their use as such is depicted in Figure 1.8. The total divergence angle θ of the diffuser is given by:

$$\theta = 2\theta_{1/2} = 2 \tan^{-1} \left(\frac{d}{2f} \right) = 2 \tan^{-1} \left(\frac{1}{2F/\#} \right), \quad (\text{Eq 1.1})$$

where $\theta_{1/2}$ is the divergence half angle, d is the diameter of the lenslet, f is the focal length of the lenslet, and $F/\#$ is defined as f/d . Most lenslet arrays are fabricated on a flat substrate [6, 30] so one side of the lens is planar while the opposite side is curved with radius of curvature R . When this is the case, the focal length of the lenslet can be calculated as:

$$f = \frac{R}{n_0 - n_g}, \quad (\text{Eq 1.2})$$

where n_g is the refractive index of the lenslet material and n_0 is the refractive index of the medium the array is immersed in (typically air). This means that the divergence angle of the lenslet array can be controlled by modifying the diameter, radius of curvature, or material of the

lenslets. As an example, a lenslet array with $d = 100 \mu\text{m}$, $R = -200 \mu\text{m}$, $n_0 = 1.5$ and $n_g = 1.5$ will have a focal length of $f = 400 \mu\text{m}$ and total divergence angle of $\theta = 14.25^\circ$.

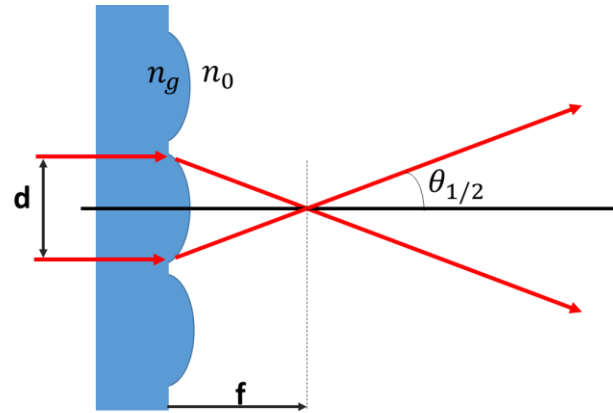


Figure 1.8. Lenslet array in a diffuser configuration

A lenslet array works as a homogenizer by taking the incident irradiance profile and redistributing it as a spatially uniform pattern across an observation plane in the far-field. For example, a beam with a Gaussian irradiance profile will be converted into a spatially uniform tophat irradiance profile after passing through the lenslet array. This is a useful fact because it means that this type of diffuser is not very sensitive to the properties of the incident light, including wavelength, irradiance distribution, and degree of collimation [17]. Most fabrication techniques are best suited to create square grids where each cell of the grid contains a lenslet with a square or circular boundary, thus creating a periodic structure. Lenslet geometries that do not completely fill the grid result in dead space that specularly transmits a zero order, thus lowering the transmission efficiency of the desired diffuser pattern. The amount of dead space is directly related to the fill factor of the array, which is defined as the percent coverage of the lenslets on the diffuser substrate. As Figure 1.9 shows, certain packing geometries can achieve fill factors of 100%. As will be discussed in the next section, this also has an impact of the spatial shape of the diffused light, meaning that lenslet arrays can also act as beam shapers [17].

It is also important to note that when using a coherent light source the periodic structure of the array will produce unwanted diffraction patterns on top of the diffused pattern. Note that the periodic structure can also produce aliasing/Moire effects in display applications [37].

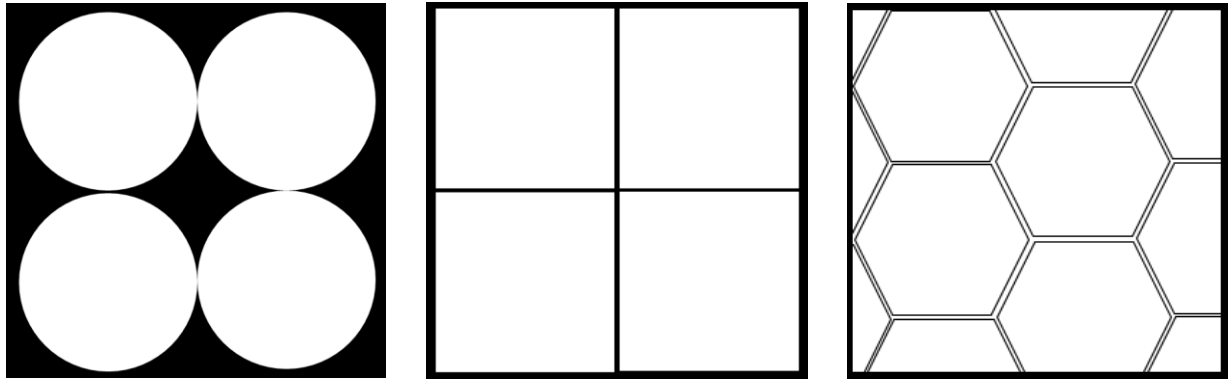


Figure 1.9. Various packing geometries of a lenslet array. Black areas depict dead space. A regular array of circular elements (left) cannot produce a fill factor of 100% while a regular array of square elements (center) or hexagonal elements (right) can. Element shape determines the shape of the diffused beam.

1.8 Engineered Diffusers

In 1997, Glockner and Goring [41] proposed a method of reducing the diffraction grating effects of periodic microlens arrays by statistically varying the individual lenslets. They investigated how changing parameters such as relative lenslet position, height, or focal length could reduce the amount of spatial coherence in the observation plane to eliminate interference fringes. This concept was extended in the early 2000's by what is now known as RPC Photonics, Inc., and the Engineered Diffuser was introduced. Enabled by precision laser lithography techniques that allow surface features up to 100 μm in depth [39], Engineered Diffusers employ statistical variations in the surface relief patterns of microlens arrays in order to achieve nearly arbitrary spatial profiles and intensity distributions in the far-field. Each parameter described below controls a property of the diffused beam and statistically varying any of these parameters will reduce diffraction artifacts [37, 38]:

a) Lenslet Sag

Most traditional microlens arrays consist of spherical lenslets because they are the simplest to fabricate, but this is not necessarily the ideal shape for every application. In general, the surface profile Z of a lenslet can be described by the general sag equation:

$$z = \frac{Y^2}{R \left(1 + \sqrt{1 - (1 + k) \frac{Y^2}{R^2}} \right)} + A_4 Y^4 + A_6 Y^6 + \dots + A_n Y^n \quad (\text{Eq 1.3})$$

where Y is the normalized pupil coordinate, R is the radius of curvature, k is the conic constant, and A_4, A_6, \dots, A_n are the even aspheric terms. Since the sag of the lenslet determines how the rays are bent as a function of pupil position, it has a direct impact on the intensity distribution of the diffuser. In this sense, utilizing aspheric terms can provide additional degrees of freedom that contribute to better diffusion control. Examples of achievable intensity profiles include Gaussian, tophat, batwing, or other arbitrary distributions. One point worth noting is that if the sag of each lenslet varies according to a probability density function (PDF) whether by design or as a result of fabrication errors, this can have a large impact on the output intensity profile.

b) Lenslet Boundary Shape

As we saw in Section 1.7, the boundary shape of each lenslet has a direct impact on the shape of the diffused light in the far-field. Specifically, circular lenslets produce circular beam shapes, square lenslets produce square beam shapes, and so on. Variations in lenslet boundary shapes across the diffuser surface are also possible. The typical drawback of circular lenslets is the fact that they cannot achieve a 100% fill factor, however one novel aspect of the Engineered Diffuser is the ability to fill in the dead space to achieve full fill factor. This method is described in [38]

and can be observed in Figure 1.10. This means that arbitrary spatial profiles are achievable while still maintaining high transmission efficiency.

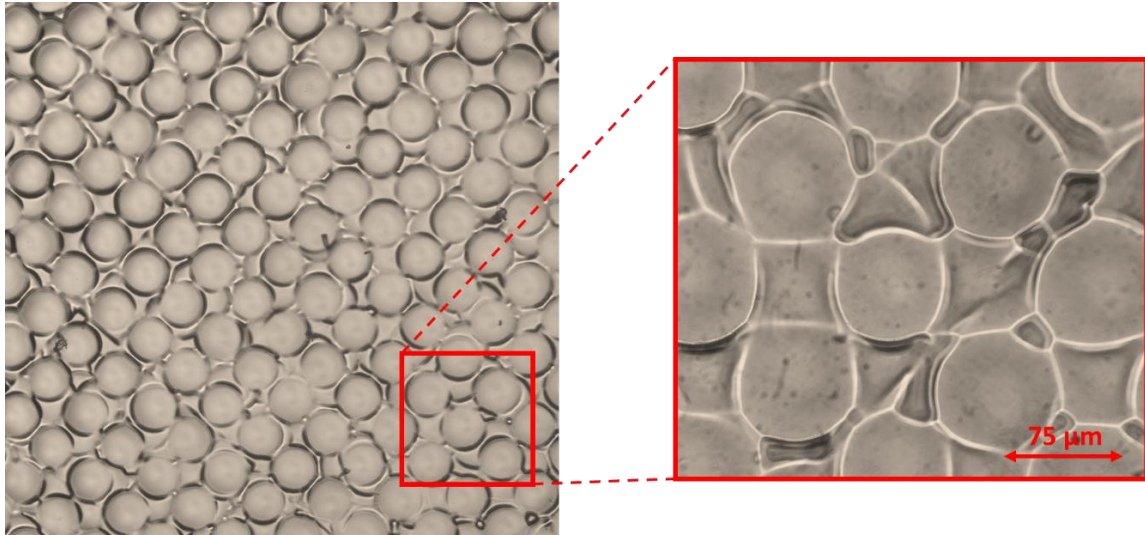


Figure 1.10. 10X (left) and 40X (right) magnified surface of a 20° circular Engineered Diffuser. The circular lenslet boundaries create a circular diffusion pattern. Dead space between lenslets is filled in to increase transmission efficiency.

c) Spatial Distribution of Lenslets

When aliasing or Moire fringes are a problem, such as in a display screen application, the periodic structure of a lenslet array must be changed to a random arrangement. This can be achieved in an Engineered Diffuser by adjusting the spatial distribution of each lenslet. This includes randomizing the center location of each lenslet and/or the size of each lenslet boundary. Additionally, the axial position of each lenslet can be modified by adding a piston offset, which primarily improves diffusion uniformity [38, 41].

Due to the numerous degrees of freedom available in their design and the fact that they are refraction based, Engineered Diffusers provide flexibility in beam shaping and intensity distribution capabilities while remaining fairly insensitive to the properties of the incident beam. This includes coherent or incoherent beams, monochromatic or white light sources, and Gaussian

or uniform incident irradiance profiles. However, there is one property of the incident light that Engineered Diffusers (and microlens arrays in general) are very sensitive to: the incident angle of the beam.

As with any lens, the microlenses that construct the diffuser surface suffer from aberrations [6, 7]. The result is a skewing effect in the diffusion pattern that can be undesirable. As can be seen in Figure 1.11, the measured output intensity profile of a 20 degree circular tophat diffuser from RPC shows how the tophat profile becomes asymmetric when the angle of incidence increases from 0° to 20°.

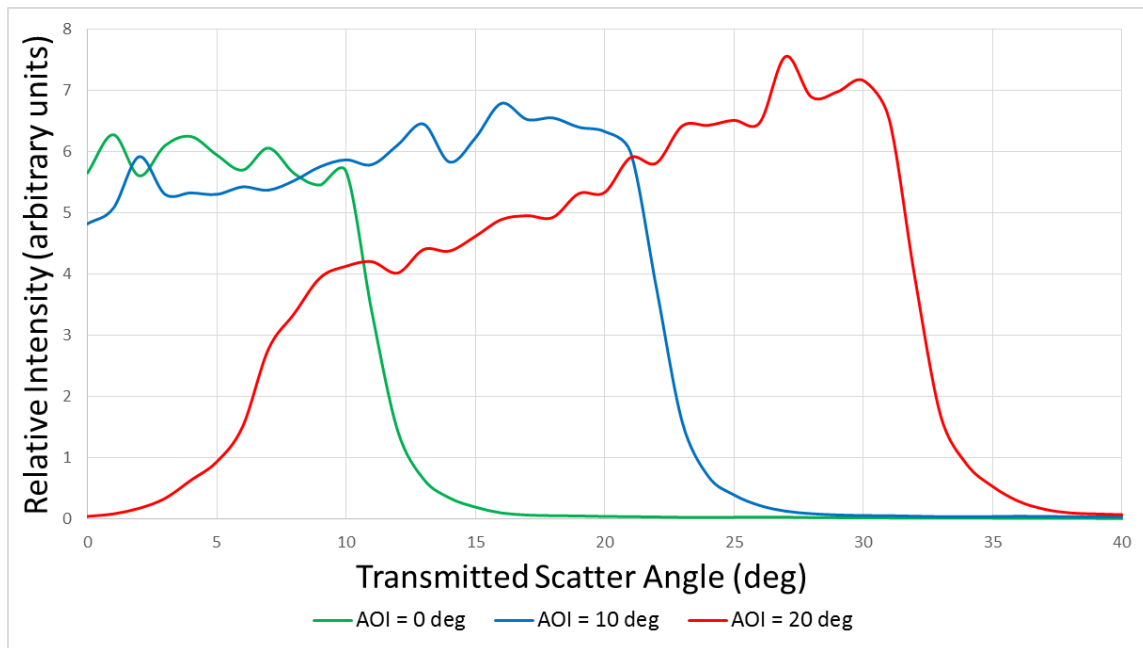


Figure 1.11. Measured intensity as a function of AOI for EDC20 RPC Diffuser [23].

To demonstrate this effect further, the surface profile of a single lenslet was measured on a white light interferometer and then modeled in Zemax. Figure 1.12 shows how the light distribution is uniform when the lens is illuminated on-axis, but the pattern becomes skewed as the angle of incidence increases mainly due to the aberrations (primarily coma and astigmatism) of the lenslet. For lenslets with steep surface profiles, total internal reflection can also play a role

in creating asymmetric diffusion patterns because portions of the incident beam will not be transmitted through the diffuser.



Figure 1.12. Simulated RPC EDC20 lenslet performance for 0°, 15°, and 30° AOI. Off-axis performance is dominated by coma and astigmatism.

1.9 Diffuser Summary

Table 1.1 below provides a summary of the diffuser devices described in this chapter. Diffractive diffusers are discussed in Chapter 3. Note that these are typical values based on theoretical approximations or performance data from commercially advertised devices. Actual performance will vary depending on the design and application conditions of each device including beam size, wavelength, AOI, coherence, collimation, input irradiance profile, fabrication accuracy, temperature, etc.

Diffuser Name	Type	Refractive or Diffractive?	Intensity Profile	Spatial Profile	Transmission Efficiency
Ground Glass	Surface	Refractive*	Gaussian	Circular	70-90%
Opal Glass	Volume	Refractive*	Lambertian	Circular	20-40%
Plastic	Volume	Refractive*	Gaussian or Lambertian	Circular	Up to 85%
Micro-Prisms	Surface	Refractive	Various	Various	>90%
Holographic Diffuser	Surface or Volume	Diffractive	Gaussian	Circular	Depends on AOI and wavelength
Light Shaping Diffuser	Surface or Volume	Refractive*	Gaussian	Circular or Elliptical	>85%
Engineered Diffuser	Surface	Refractive	Various	Various	>90%
Diffractive Diffuser	Surface	Diffractive	Various	Various	75-95% at design wavelength

Table 1.1. Summary of Diffusers

*Although these diffusers primarily refract light in random directions, they impart random phase variations onto the incident wavefront which results in noticeable diffraction effects (speckle) when illuminated by coherent light.

CHAPTER 2

Diffusers in Laser Spot Trackers

2.1 Diffusers and Lenses

Figure 2.1 depicts a standard diffuser illuminated by a collimated, on-axis beam. The beam size D at the observation plane is simply given by:

$$D = 2L \tan \theta_{1/2} \quad , \quad (\text{Eq 2.1})$$

where L is the distance from the diffuser to the observation plane and $\theta_{1/2}$ is the divergence half angle. The red rays in the figure are diffused rays and the black ray is the specularly transmitted ray.

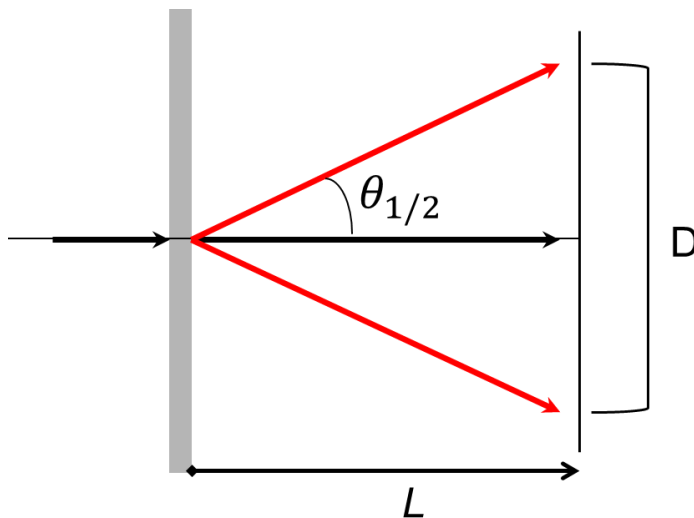


Figure 2.1. Diffuser used without lens

If a lens is placed near the diffuser the beam size at the focal plane of the lens is defined as

$$D = 2f \tan \theta_{1/2} \quad , \quad (\text{Eq 2.2})$$

Where f is the focal length of the lens being used. In this configuration the black, specularly transmitted rays determine the image location of the lens and the red, diffused rays bound the maximum diffused spot size (see Figure 2.2). The relative distance between the diffuser and lens is not important as long as the lens is large enough to gather all of the rays diverging from the diffuser.

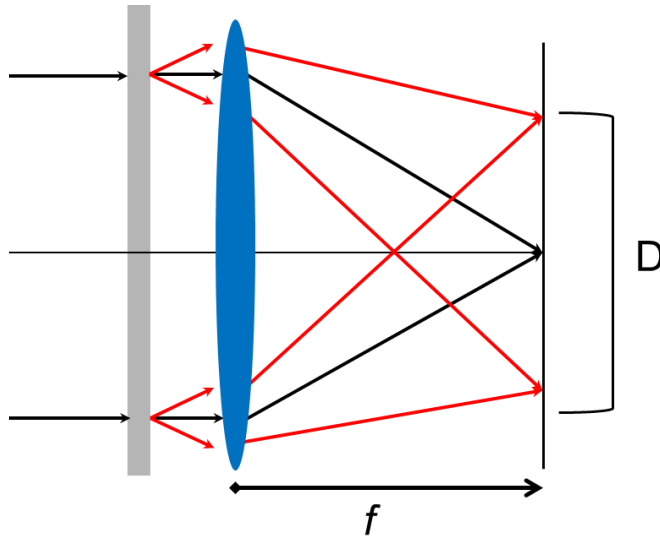


Figure 2.2. Diffuser used with lens

2.2 Laser Spot Trackers

One unique application of diffusers is in laser spot tracking systems. A laser spot tracker is a device that receives laser energy from a target in order to determine its angular position. Applications include optical disc readers [42], laser range finders, telecommunication, metrology, and guidance systems [43]. As depicted in Figure 2.3, these systems are used to track laser energy being emitted, scattered or reflected from a target in order to determine the target's azimuth and elevation angles (α , β) relative to the tracker. A laser source, sometimes referred to as the designator, can be used to illuminate the desired target to be tracked and a portion of the incident beam makes its way to the spot tracker which typically consists of focusing optics that

concentrate the energy onto a quad-cell detector. The angular position of the target is determined by the distribution of the focused laser energy on the quadrants of the detector as shown in Figure 2.4. When the spot is centered exactly on the detector this means the target is precisely lined up with the tracker. This position is sometimes called boresight. When the target is not directly on boresight with the tracker the laser spot is displaced laterally on the quadrants. Since the intent of the tracker is to look straight at the target, this is registered as a position error that can be quantified by the proportional amount of energy on each quadrant given by Eq 2.3a and Eq 2.3b [14]:

$$\Delta x = K \frac{(B+D)-(A+C)}{A+B+C+D} \quad (\text{Eq 2.3a})$$

$$\Delta y = K \frac{(A+B)-(C+D)}{A+B+C+D} \quad (\text{Eq 2.3b})$$

where Δx is the horizontal position of the laser spot centroid, Δy is the vertical position of the laser spot centroid, K is a scaling factor related to the size of the beam on the detector, and A , B , C , D are the electrical signals produced by each respective quadrant. These equations determine what is known as the Spatial Transfer Function (STF) of the tracking system. The ideal transfer function has a linear slope over the field of view of the system. This is discussed further in Section 4.4. The angular position of the target can now be determined based on the position of the spot and the known focal length, f , of the focusing optics [14]:

$$\alpha = \tan^{-1}\left(\frac{\Delta x}{f}\right) \quad (\text{Eq 2.4a})$$

$$\beta = \tan^{-1}\left(\frac{\Delta y}{f}\right) \quad (\text{Eq 2.4b})$$

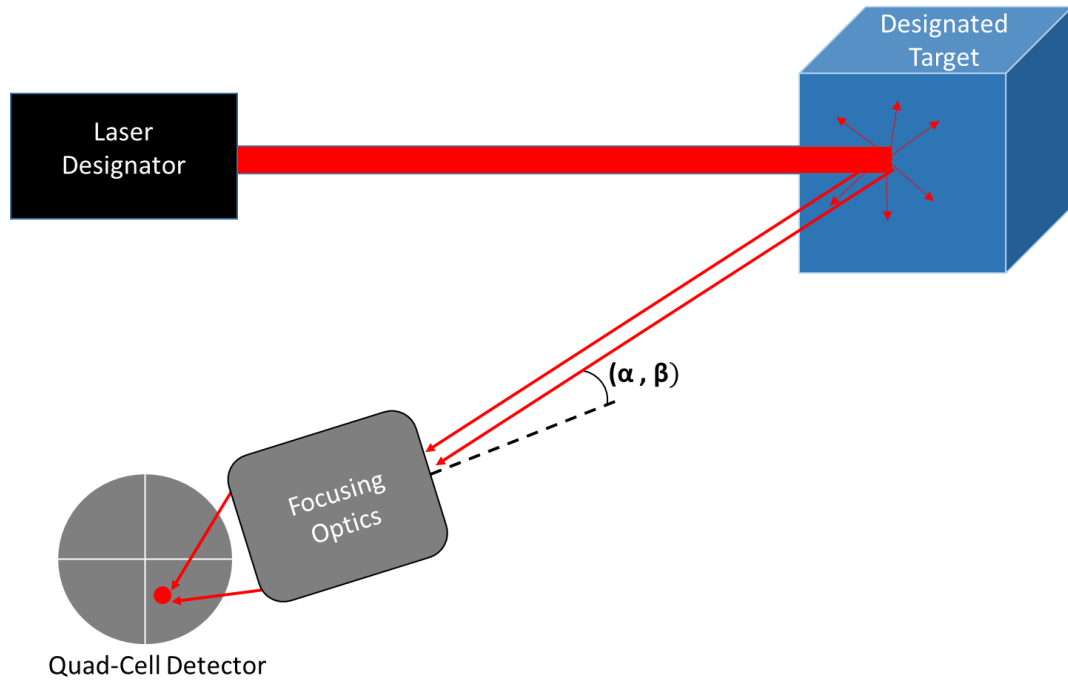


Figure 2.3. Laser Spot Tracker Geometry

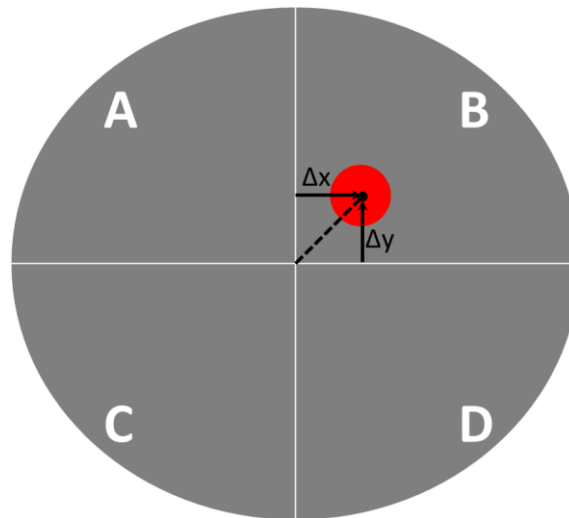


Figure 2.4. The angular position of the target can be determined by the Δx and Δy offset of the focused laser spot on the quadrants of the detector

The idea of using laser spot trackers to locate and follow a target has been around since the 1960's. Original designs relied on an optical system to focus the target signal to a tightly focused spot on a quad cell detector in order to provide angular direction information to the

system. However, in applications where the target is being tracked over long distances, air turbulence in the atmosphere can lead to rapid fluctuations in the tilt of the incident wavefront [15]. These cause the focused laser spot to jitter across the detector quadrants, making tracking very difficult. Additionally, aberrations of the focusing optics can produce misshaped or uneven energy distributions within the laser spot that can confuse the tracking algorithms that use Equations (2.3a) and (2.3b).

One early solution to the atmospheric turbulence problem was to intentionally introduce defocus to the system, causing the laser spot to expand at the detector so that it covers more area on each quadrant, thus averaging out the jitter effect. However, this solution suffers from a slightly different, but related, problem known as scintillation. The scintillation effect is caused by refractive index gradients in the atmosphere that lead to non-uniform energy distributions across the entrance pupil of the tracker [9, 15]. Since each portion of the defocused laser spot corresponds to a portion of the entrance pupil, scintillation causes a rapid blinking effect in the spot which also makes tracking difficult.

A different idea proposed by Conrad [16] was to place a square binary diffraction grating near the focusing optics to produce an array of diffraction spots in the detector plane. The position of the brightest spot would correspond to the angular position of the target. This solution averages out the effects of scintillation and spot non-uniformities, but the downside is that it requires auxiliary detectors around the quad-cell detector to detect the higher diffracted orders, which adds cost and complication to the design.

2.3 Diffusers in Laser Spot Trackers

A solution to both the scintillation and uniformity problems above was proposed by Jenkins and Taylor [8] in 2005 and Layton [9] in 2006 where a diffuser is used in conjunction

with the focusing optics and quad-cell detector. One possible configuration of this is depicted in Figure 2.5, where the diffuser is at or near the entrance pupil of the system. Note how the laser spot has expanded on the detector plane relative to Figure 2.3, meaning the system is insensitive to jitter from atmospheric turbulence. The difference, however, is that the diffuser takes the incident energy, regardless of how it is distributed across the entrance pupil, and maps it to a uniformly diffused spot. This solves the scintillation problem. Additionally, since the diffuser creates a homogeneous spot of energy it also solves the non-uniformity problem. This also has the added benefit of making the optical system less sensitive to defocus and other aberrations, making the design simpler and easier to assemble.

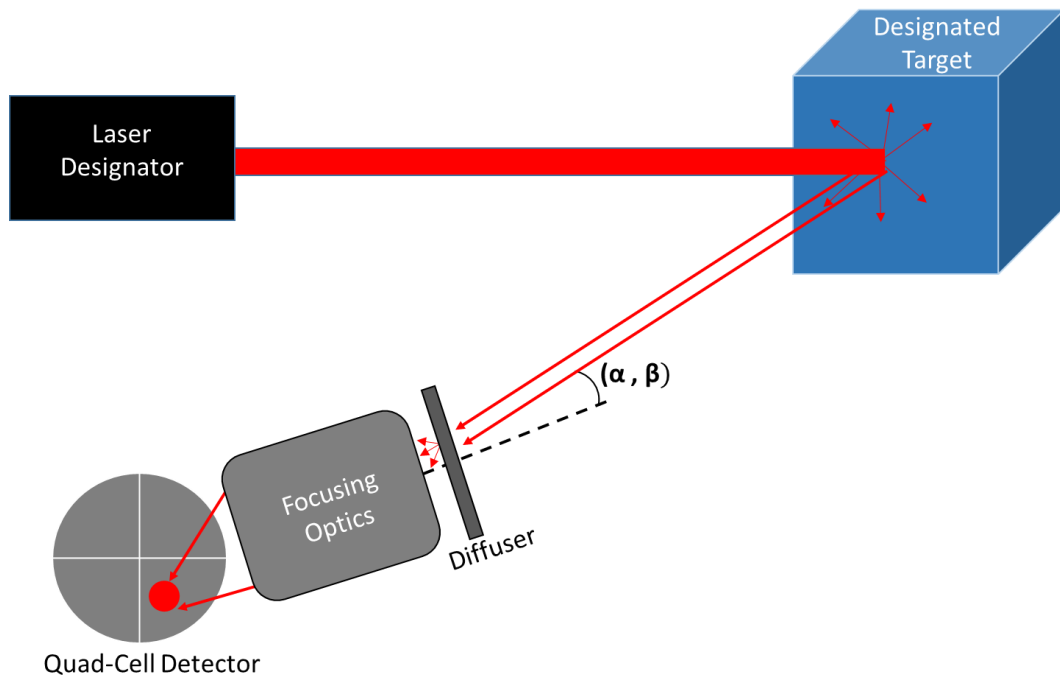


Figure 2.5. Diffuser added to Laser Spot Tracker System

In their proposed design, Jenkins and Taylor suggested using a Light Shaping Diffuser from Physical Optics Corporation, a periodic lenslet array, an Engineered Diffuser from RPC, or even replicating a diffusing structure onto the surface(s) of the focusing optics to serve as the diffuser element. Similarly, Layton specifically suggested using an Engineered Diffuser because

of its flexibility to produce various spot shapes (circle, square, ellipse, etc.) and its ability to create a uniform irradiance profile, which works best for tracking algorithms [9,14, 43].

However, what Layton did not account for is the fact that, as we learned in Section 1.8, the Engineered Diffuser microlenses themselves suffer from aberrations and this causes the diffused spot to become skewed as the angle of incidence increases. Figure 2.6, which is taken from Layton's patent, shows the ideal diffuser performance. The uniform, square diffused pattern remains constant as it travels across surface of the detector as a function of field angle, making it very easy to track the target. In reality, the diffused pattern looks something like Figure 2.7, which shows the actual diffusion pattern obtained from an EDC 20 diffuser from RPC at various angles of incidence. The skewing of the spot complicates the tracking algorithms and this becomes a limiting factor in the maximum FOV that can be achieved by such a system.

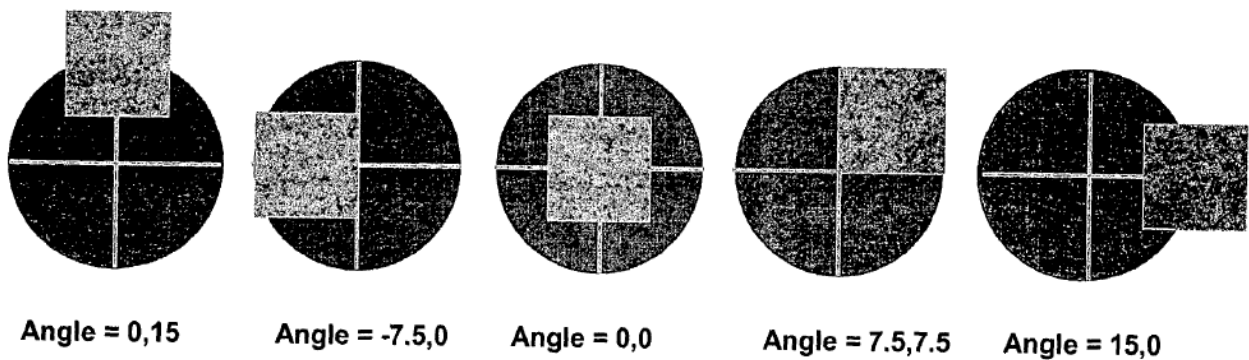


Figure 2.6. Ideal Laser Spot Tracker Diffuser Performance.



Figure 2.7. Actual Performance of RPC EDC 20 at AOI = 0° (left), 15° (center), and 30° (right)

It therefore would be advantageous to use a diffuser that is able to achieve arbitrary spot shapes and uniform irradiance profiles without suffering from off-axis aberrations that skew the irradiance profile of the spot. A review of the diffusers described in Chapter 1 shows that none of them can meet this criteria. This thesis introduces an alternative diffusing element that can solve these problems while maintaining the basic functionality of other diffusers within the context of a laser spot tracking system.

2.4 Diffractive Diffusers in Laser Spot Trackers

Most laser spot trackers operate with coherent, monochromatic illumination of known wavelength while using focusing optics of known $F/\#$ and focal length. As described in Section 2.2, Conrad utilized these parameters by using a diffractive grating near the focusing optics to create an array of laser spots in the detector plane to mitigate atmospheric scintillation. Now if we replace the diffractive grating with a grayscale diffractive optical element known as a computer generated hologram (CGH), we can produce a far field diffraction pattern that matches the laser spot properties we desire (i.e. arbitrary shape, uniform irradiance profile, no off-axis skewing). This means we can achieve a laser spot tracker that utilizes a single quad-cell detector, does not suffer from scintillation, does not suffer from spot non-uniformities, and works over a wider FOV. Chapter 3 discusses this idea in further detail.

CHAPTER 3

Diffractive Diffuser Design

3.1 Computer Generated Holograms

A conventional hologram is created by recording the interference pattern of two wavefronts: one coming from the object of interest and the other coming from a reference beam. Once the pattern is recorded, a reconstruction beam incident on the hologram will recreate the object pattern for the observer in the form of a real or virtual image (depending upon the configuration of the construction and reconstruction geometries). Alternatively, a computer generated hologram (CGH) uses prior knowledge of the incident wavefront and the desired observation pattern to numerically calculate the hologram pattern to be fabricated based on diffraction calculations for near field (Fresnel) or far field (Fraunhofer) operation (see Figure 3.1). Once fabricated, the CGH serves as a thin surface-relief hologram that imparts the correct amount of phase to the incident wavefront to achieve the intended irradiance pattern in the observation plane. There are several advantages to this method over traditional holography which include the ability to model/optimize the pattern, elimination of the hologram recording step, and perhaps most importantly is the fact that a CGH can create arbitrary output wavefront distributions. This means that the hologram pattern can be designed without the physical object ever existing – something that cannot be done with conventional holograms [19]! In certain situations, using a CGH allows a lot of additional capabilities to a designer that are otherwise impractical or impossible. As a result, CGHs have become common tools in applications such as

beam shaping, beam homogenizing, laser fan-out gratings, optical interconnects, and test nulls for aspheric surfaces.

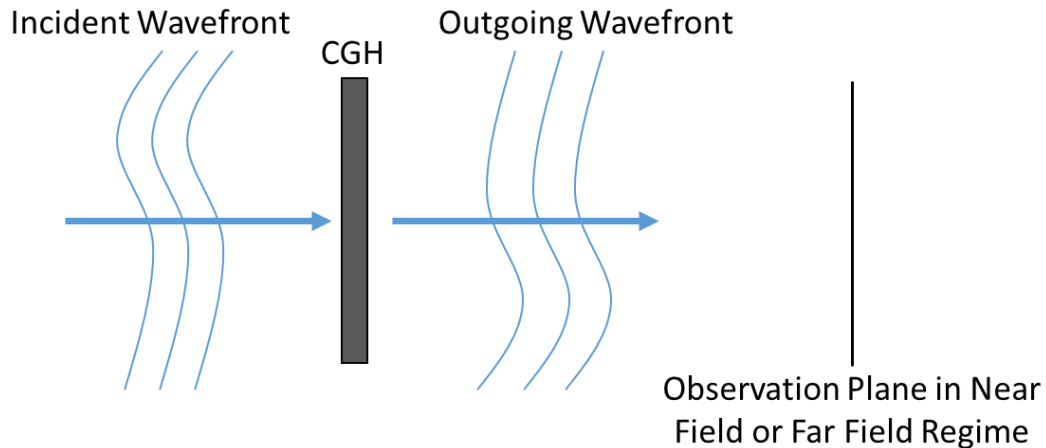


Figure 3.1. Basic Operation of CGH

Since the phase profile of a CGH is numerically calculated (as opposed to analytically calculated like a diffraction grating), there are numerous algorithms that can be used to obtain a similar result. As discussed in [18] and [25], methods include iterative Fourier transform (IFT) algorithms, steepest descent algorithms, genetic algorithms, random search algorithms, and others. An IFT algorithm known as the Gerchberg-Saxton (GS) algorithm is the most commonly used in the design of CGHs that are intended to work in the far field and it is what was chosen for this project.

3.2 Gerchberg-Saxton Algorithm

The GS algorithm utilizes the Fourier transform relationship that exists between a diffractive surface and its far field irradiance pattern. If the irradiance of the field incident upon the CGH surface is known and the observation plane is a long distance away, then the desired irradiance of the field at the observation plane is related to the incident field by a Fourier transform and there must be a phase profile at the CGH plane that relates the two. Since

irradiance is the square modulus of field amplitude, we do not care about how the CGH modifies the phase of the incident wavefront as long as it results in the intended output irradiance profile. This means that the GS algorithm can iterate back and forth between the CGH plane and observation plane, modifying the phase of the field until a stable solution is reached that relates the two irradiance profiles. The iterative process is depicted in Figure 3.2. In the figure we are assuming the CGH plane is being illuminated by a uniform amplitude plane wave, but this could be changed to any arbitrary illumination scenario such as a Gaussian laser beam, for example. Additionally, the figure shows the amplitude in the observation plane is a circular tophat pattern, which is ideal for the laser spot tracking application of this project.

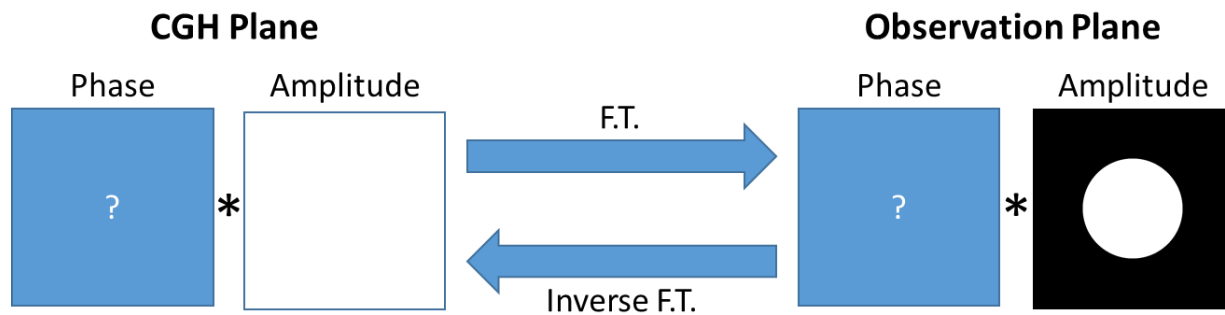


Figure 3.2. The Gerchberg-Saxton algorithm involves resetting field amplitude at the CGH and observation planes while propagating the random phase component until a stable solution is found.

In practice, the algorithm typically starts at the observation plane (Fourier transform plane) where the user inputs the amplitude of the pattern they would like to produce. Next, a random phase distribution is applied across the plane and multiplied by the pattern amplitude as a starting point for the calculation. From there the inverse Fourier transform is applied to obtain the amplitude and phase at the CGH plane. At this point the amplitude at the CGH is set to the incident amplitude (such as a uniform plane wave) while the phase is left unchanged. Next, the Fourier transform is taken to go back to the observation plane, the amplitude is reset to the

desired pattern, the phase is maintained, and the process is repeated. This goes on until the phase converges to a reasonable and stable result.

3.3 Design of a Diffractive Diffuser

A CGH that transforms a beam into a uniform pattern is often referred to as a beam shaping CGH or a diffractive diffuser because it has a well-defined divergence angle (angular spectrum to be more precise) and it maps the incident energy to a diffused spot. For this project, a diffractive diffuser was designed to produce a 10° uniform circular spot to be used in a simulated laser spot tracker system. The parameters for this design were conveniently chosen based on readily available fabrication and testing equipment:

- Design Wavelength = 532 nm (for ease of testing)
- Minimum CGH Pixel Size = $2.1 \mu\text{m}$ (limitation of fabrication tool)
- Diffuser Spread Angle = $\pm 5^\circ$
- Diffuse Irradiance Pattern = Circular Top-hat
- Diffuser Diameter = 1" (for ease of testing)
- Diffuser Substrate = Glass
- Diffuser Material = Positive Photoresist ($n = 1.609 @ 532 \text{ nm}$)

These parameters were entered into a design program known as Optiscan [45], which takes an input bitmap file of the desired far field pattern (a uniform circle in this case) and runs the GS algorithm for a designated number of iterations. As shown in Figure 3.3, this program also allows the user to input the physical size of the CGH to be fabricated, the pixel size of the fabricating device, the diffusion angle, and the number of quantization levels of the pattern. Once the program begins to run it displays the signal-to-noise ratio (SNR) of the CGH pattern (Figure 3.4) and once all of the iterations are complete it displays the simulated output pattern (Figure 3.5). Finally, the program produces a grayscale bitmap pattern of the CGH surface to be fabricated (Figure 3.6). As discussed in the next section, this bitmap is used by the fabrication machine to produce the correct exposure pattern on the photoresist layer.

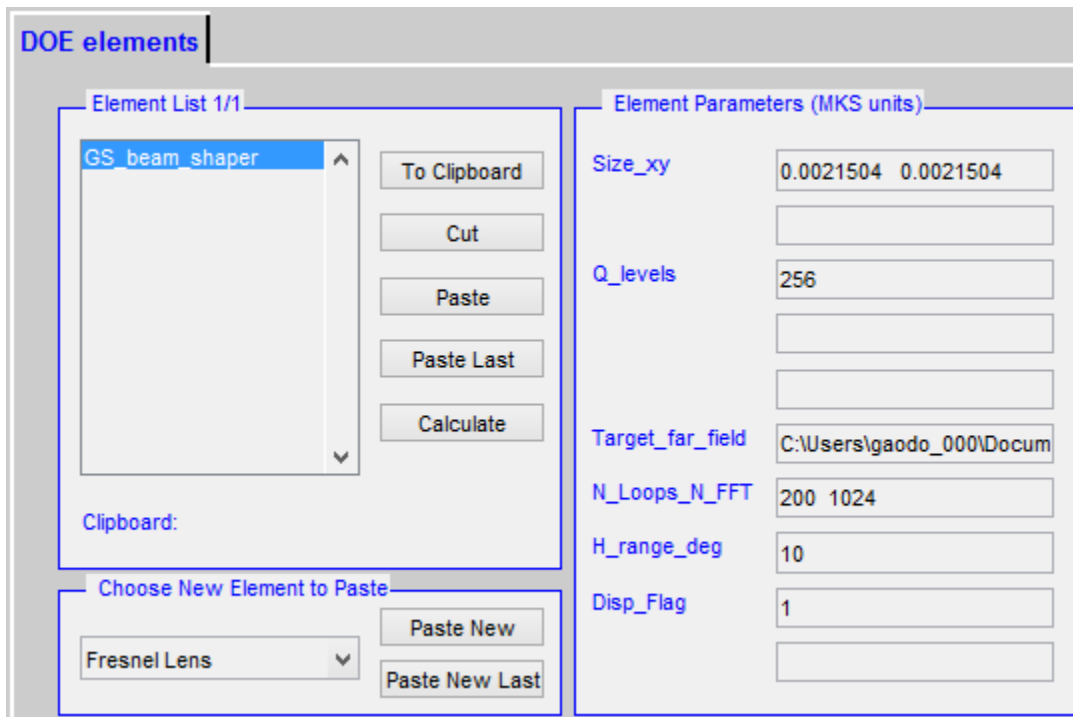


Figure 3.3. Parameters used in OptiScan to design the CGH

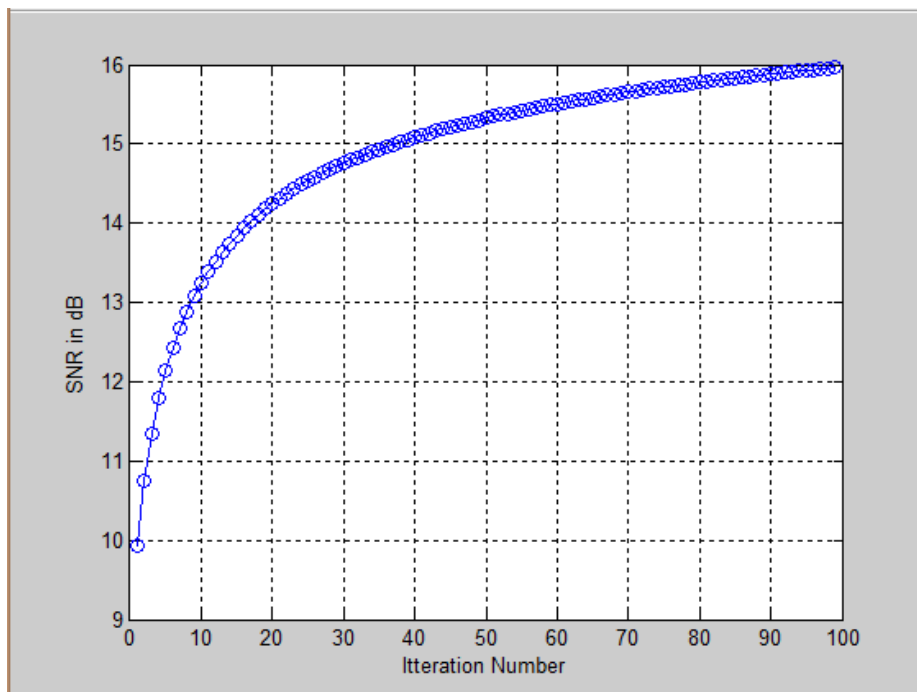


Figure 3.4. SNR of CGH pattern vs iteration number

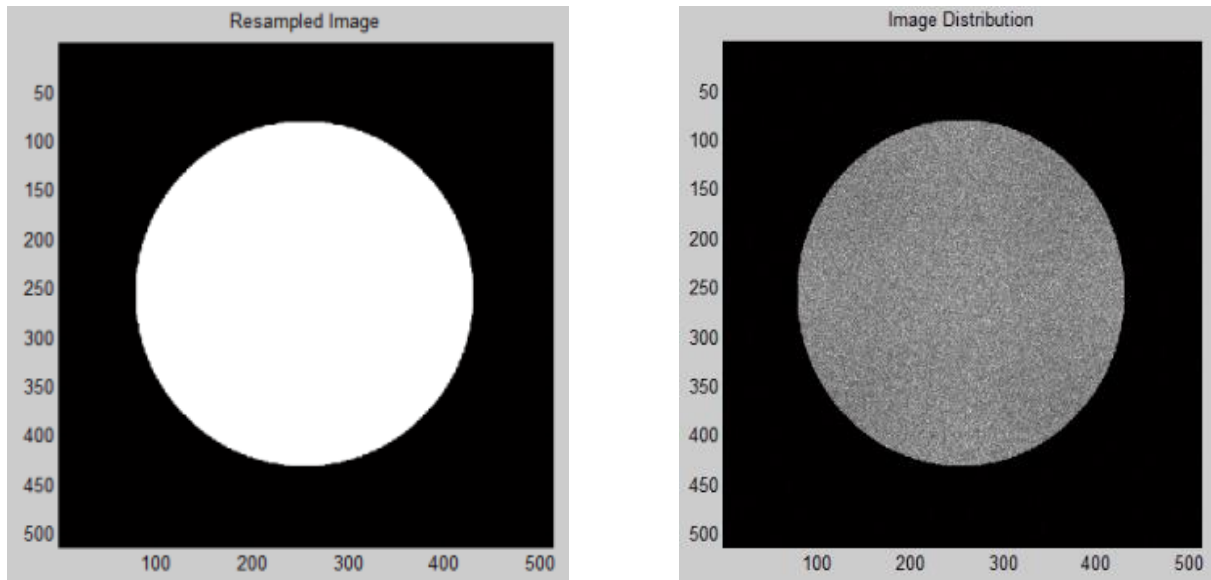


Figure 3.5. Input image (left) and simulated far field pattern produced by CGH (right). Dimensions are pixels.

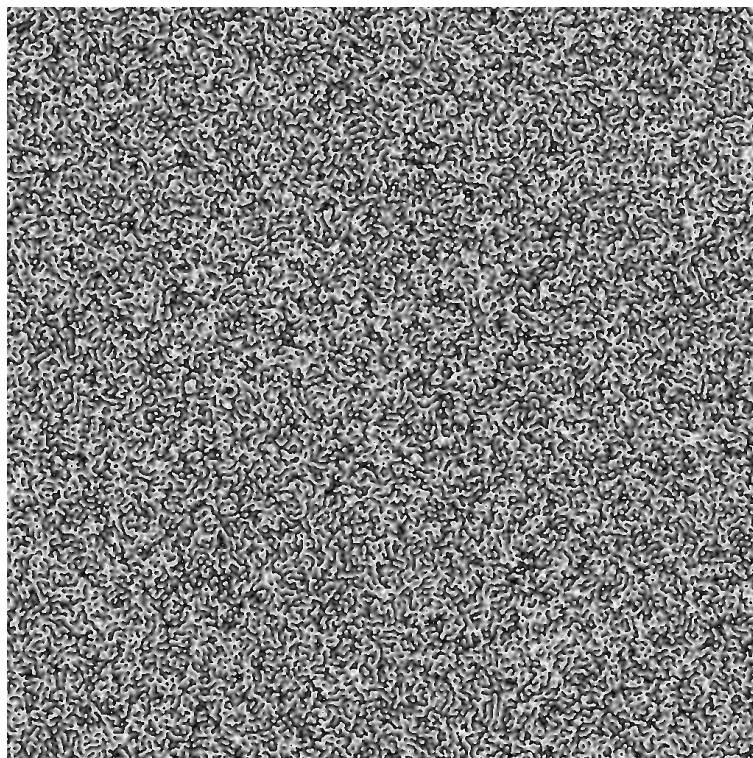


Figure 3.6. CGH pattern produced by Optiscan.

Now that the pattern is produced, the physical height needs to be determined. Using a blazed phase transmission grating as an example, 100% diffraction efficiency can be directed into a single diffracted order m by imparting a maximum optical path difference (OPD) of $m\lambda$ to the

illuminating beam. If we assume $m=1$ and the grating is in air, this corresponds to a maximum physical grating depth given by

$$h = \frac{\lambda}{n_g - 1}, \quad (\text{Eq 3.1})$$

where n_g is the refractive index of the grating. This same concept applies to a diffractive diffuser where we want all of the energy to be directed to the first diffraction order. We know that n_g is 1.609 at the 532 nm wavelength, which means that the optimal etch depth for this diffuser is 0.874 μm .

3.3 Limitations of Design

The maximum divergence half angle of a CGH is determined by the minimum feature size of the physical pattern that will be produced. This is given by [18]

$$\theta_{max} = \sin^{-1}\left(\frac{\lambda}{2AU}\right), \quad (\text{Eq 3.2})$$

where AU is the minimum feature size. For the parameters listed above, $AU = 2.1 \mu\text{m}$ and $\lambda = 532 \text{ nm}$, which means that the CGH can achieve a maximum divergence half angle of 7.28° . This value is also affected by the number of quantization levels used to produce the surface profile of the diffuser [30]. Thus, the maximum achievable divergence angle of a diffractive diffuser is highly dependent on the fabrication equipment being used.

CHAPTER 4

Diffraction Diffuser Fabrication, Testing, and System Performance

4.1 CGH Fabrication Process

The samples to be printed were prepared per the following steps:

- 1.) Score and break Corning microscope slides into approximately 1x1 inch squares.
- 2.) Clean glass squares using isopropyl alcohol followed by spraying with dry nitrogen.
- 3.) Spin coat photoresist onto the glass substrates at a thickness of approximately 5 μm .
- 4.) Soft bake the samples for 3 minutes at 115° C to prepare them for exposure.

After preparing, the sample was placed on the motorized stage of the College of Optical Science's maskless lithography tool (MLT). The MLT uses an acousto-optically modulated, i-line argon ion laser that is capable of producing 2.1 μm feature sizes [46]. The machine is controlled through a LabVIEW interface that controls the modulator and the sample stage to print the desired pattern, which is input as a bitmap file. Once the photoresist has been adequately exposed, the sample is puddle developed for about 2 minutes in a 3:1 mixture of DI water heated to 29° C and OPD 4262 developer.

4.2 CGH Testing Setup

After fabrication, the CGH was tested using a setup consisting of a spatially filtered, collimated 532 nm laser beam large enough to completely fill the CGH pattern. The setup allowed precise control of the AOI of the beam so off-axis measurements could be made. In a

configuration similar to Figure 2.2, a lens was placed directly behind the CGH and an imaging detector was placed at the focus of the lens. This was the primary configuration used. In the configuration shown in Figure 4.1, there is enough room between the lens and detector that the CGH can be placed between them, which produces a scaled irradiance pattern at the detector [26].

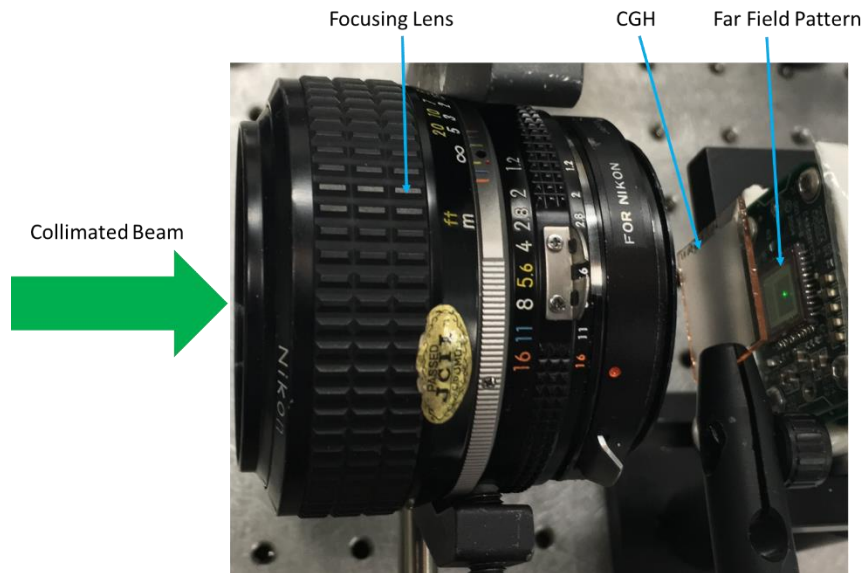


Figure 4.1. Secondary CGH testing configuration

4.3 Off-Axis Behavior of Diffractive Diffusers

The vast majority of diffractive diffusers are designed with the intent of being illuminated by an on-axis laser beam. Primary examples include single or multi-mode laser beam shaping, laser homogenizing, and laser lithography [18, 44]. As a result, the off-axis performance of these devices is typically not discussed. There are two primary effects of using oblique illumination with a diffractive diffuser:

a) Change in Optical Path Length

As discussed in Chapter 3, diffractive diffusers are usually fabricated so that normally incident light of a specific wavelength will experience an optical path difference (OPD) of λ , ideally producing 100% diffraction efficiency into the diffused pattern. When the light is incident upon

the diffuser at an off-axis angle, the optical path difference (OPD) of the beam increases. This results in lower diffraction efficiency and makes the zero order more noticeable. As depicted in Figure 4.2, ray A and ray B are incident upon the diffractive structure of depth h at an angle of incidence θ . The optical path lengths (OPL) of each ray are summarized as

$$OPL_A = n_g \frac{h}{\cos\theta} , \quad (\text{Eq 4.1})$$

$$OPL_B = \frac{h}{\cos\theta} . \quad (\text{Eq 4.2})$$

This leads to an optical path difference of

$$OPD = OPL_A - OPL_B = (n_g - 1) \frac{h}{\cos\theta} , \quad (\text{Eq 4.3})$$

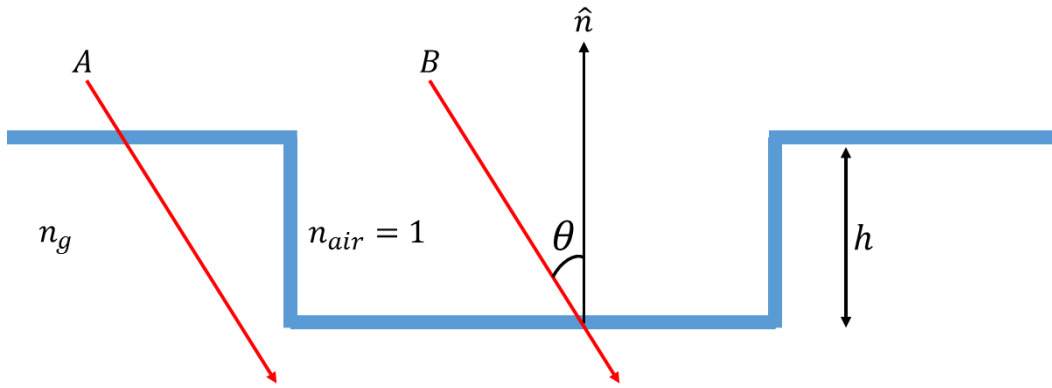


Figure 4.2. Off-Axis illumination of diffractive structure

b) Elongated Diffusion Pattern

Diffraction from a CGH can be understood by looking at the grating equation:

$$n_g \sin \theta_g - n_0 \sin \theta_m = \frac{m\lambda}{d} , \quad (\text{Eq 4.4})$$

Where n_g is the refractive index of the grating, θ_g is the angle of light incident upon the grating, n_0 is the refractive index of the medium after the grating, θ_m is the diffraction angle of the diffraction order m , and d is the grating period. This equation allows us to understand how a grating structure will spread the incident light. For illustration purposes, we will focus only on

the divergence of the +1 and -1 diffracted orders as a function of incident angle θ_g . As Figure 4.3 shows, when the incident angle is small the +1 and -1 orders are evenly spaced around the $m = 0$ undiffracted order.

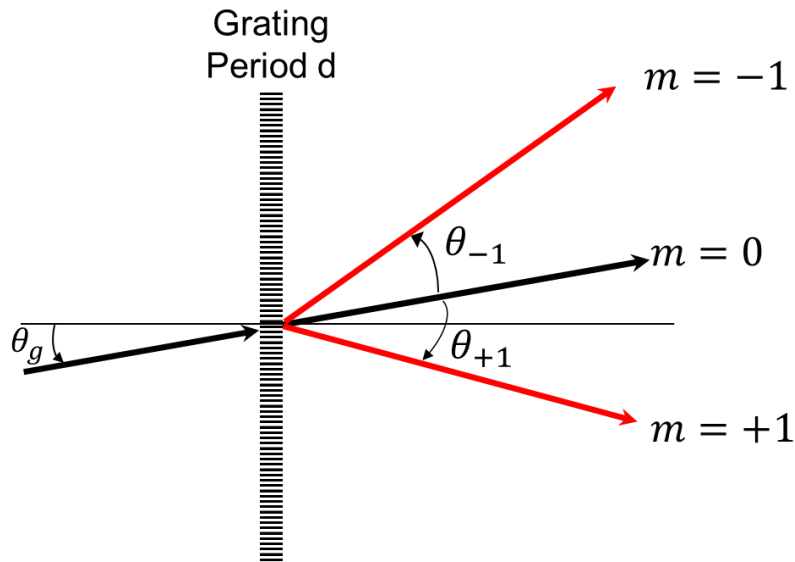


Figure 4.3. First diffracted orders from a periodic grating

However, once the angle of incidence increases, there is a non-linear separation of the diffraction orders. As can be seen in Figure 4.4, the red line representing the diffraction angle of the $m = -1$ order begins to rapidly diverge when the AOI approaches 25° , causing the separation of the two primary diffracted orders to increase until eventually the -1 order is no longer transmitted because it experiences total internal reflection (TIR). Figure 4.5 provides a visualization of the angular separation between the two orders as a function of AOI. We can see that, for this grating, the angular separation remains approximately 30° from about 0 - 10° AOI.

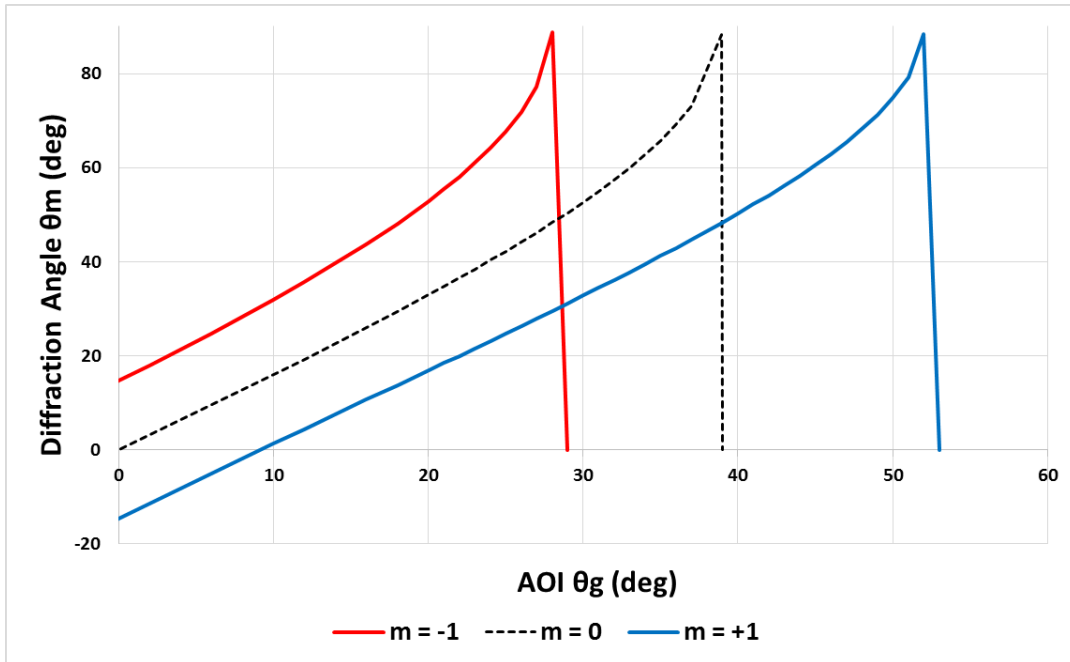


Figure 4.4. Diffraction angle vs angle of incidence for the +1 and -1 diffraction orders. The 0 order is also shown for reference. This chart assumes a grating period of $d = 2.1 \mu\text{m}$ and wavelength of $\lambda = 532 \text{ nm}$.

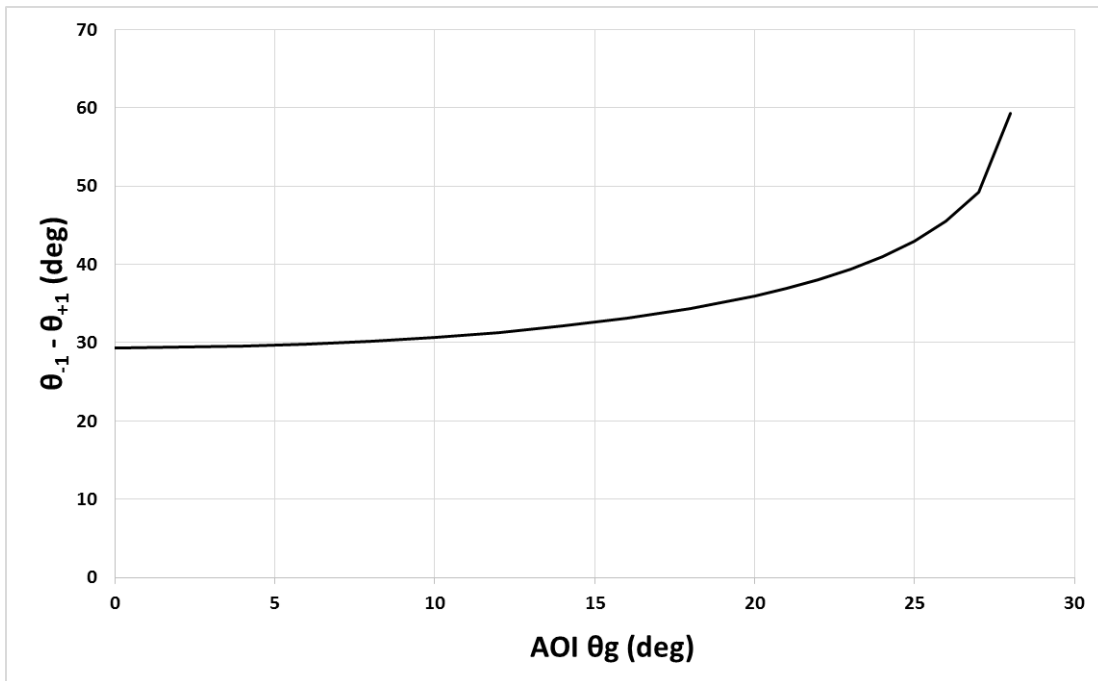


Figure 4.5. Angular separation of the +1 and -1 diffraction orders vs angle of incidence.

Up to this point we have only been describing angular separation of the diffracted orders in terms of a binary diffraction grating, but this concept enables us to understand the elongation effect that

occurs when a CGH is illuminated by an off-axis source. Figure 4.6 and Figure 4.7 show how the circular diffraction pattern created by our designed CGH becomes elliptical as the AOI increases. The pattern stretches by nearly 50% in the plane of the incident beam. Additionally, it can be seen that half of the diffused pattern becomes darker as the AOI increases, which corresponds to the -1 order experiencing TIR as we saw in Figure 4.4.

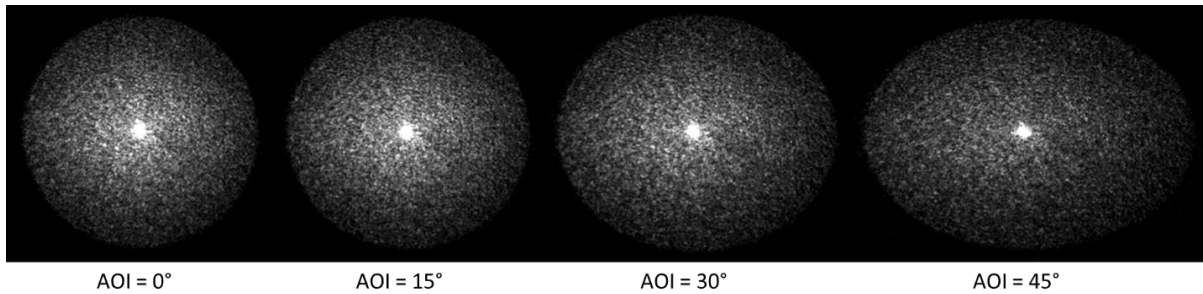


Figure 4.6. Diffused diffraction pattern stretches as the AOI increases.

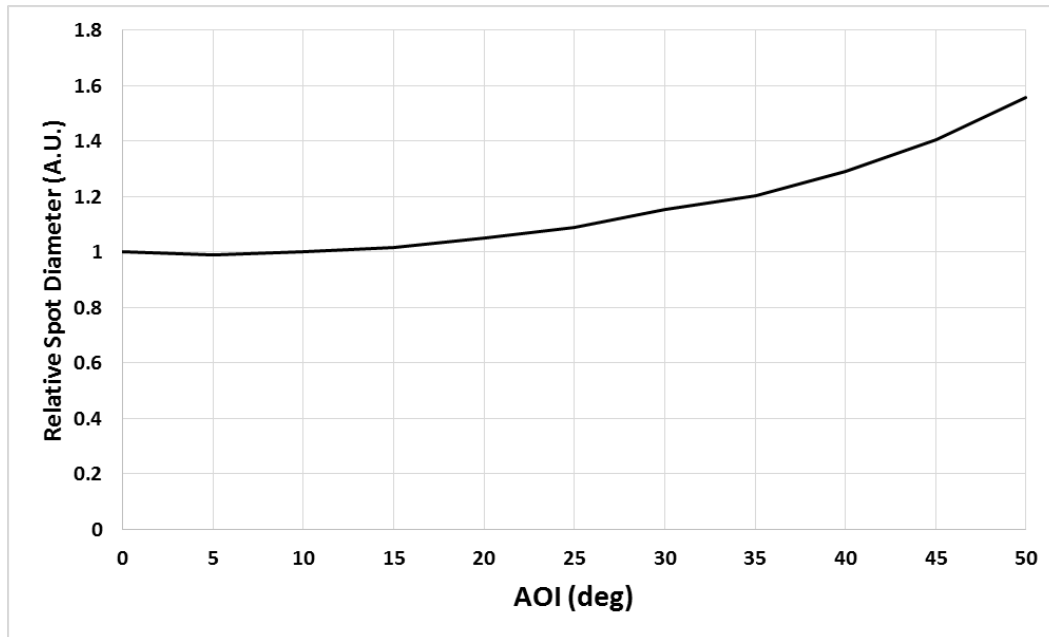


Figure 4.7. Relative spot diameter in x-dimension vs angle of incidence. The pattern stretches as AOI grows.

4.4 Spatial Transfer Function Performance

Utilizing equation 2.3b, the elevation STF was measured to understand how the off-axis behavior of different diffusers impacts system performance. As was mentioned earlier, the theoretical STF is a linear function when a uniform spot is used, but aberrations and pattern elongation cause the response to be non-linear. Figure 4.8 shows the results for an ideal uniform spot (nearly what is produced by our CGH), a Gaussian spot (such as what is produced by a Light Shaping Diffuser), a stretched Gaussian spot (this was simulated to show the effects of pattern elongation), and an aberrated spot (from the RPC EDC20 diffuser). This data would suggest that our CGH is able to achieve the best off-axis performance.

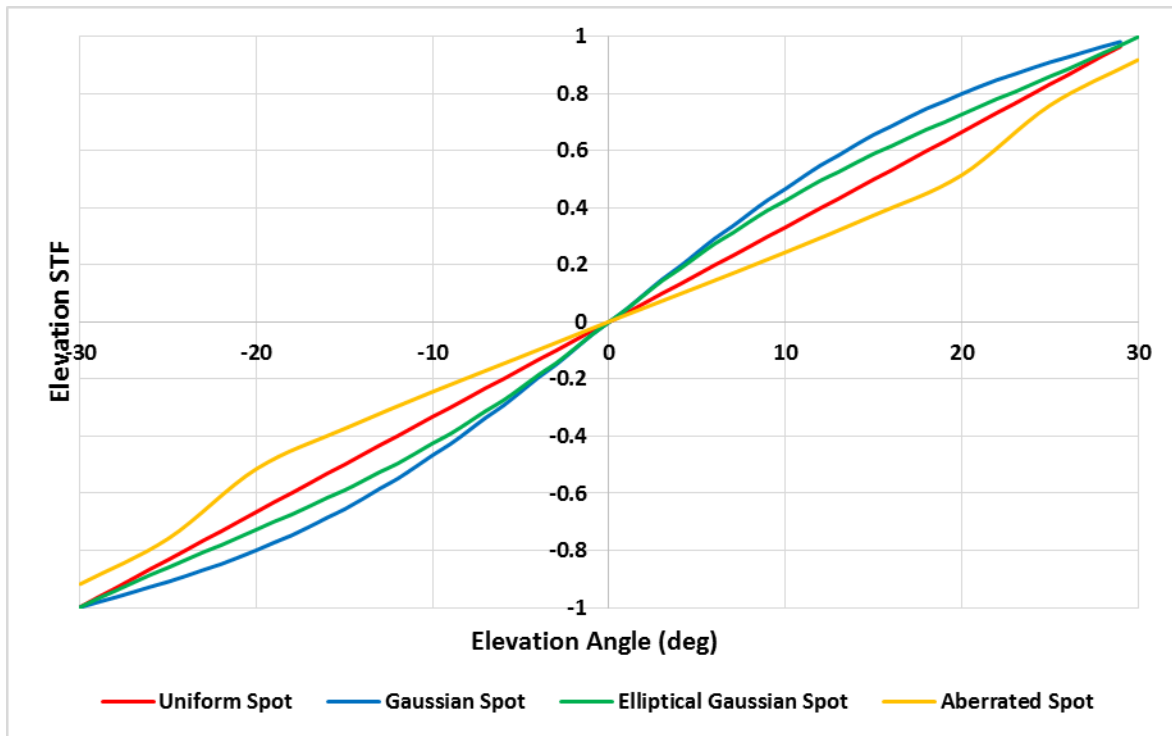


Figure 4.8. Elevation STF vs AOI for various diffuser types

CHAPTER 5

Conclusion

5.1 So Which Diffuser is the Best?

This project has discussed the benefits and pitfalls of various diffusers as it pertains to their application in systems that use coherent illumination over a wide field of view. We saw that diffusers such as ground glass and bulk diffusers are fairly insensitive to angle of incidence, but they are not very efficient, their diffusion angles cannot be well controlled, and they are limited in their ability to produce various beam shapes and intensity profiles. Similarly, we saw that Light Shaping Diffusers can achieve slightly better transmission and beam control properties, but they can only produce Gaussian intensity profiles due to the random nature of how they are fabricated. A periodic lenslet array can achieve various intensity distributions and divergence angles, but the periodic structure produces unwanted diffraction artifacts when used with coherent illumination. An Engineered Diffuser can achieve the flexibility of a lenslet array without suffering from diffraction artifacts, but the off-axis performance of both of these devices is limited by aberrations. A diffractive diffuser has the flexibility of the Engineered Diffuser in its ability to create various intensity profiles and beam shapes, but its divergence angle is limited by fabrication techniques. Additionally, the off-axis behavior of a diffractive diffuser can result in a noticeable zero order and pattern elongation. If these effects are tolerable then the diffractive diffuser may be the best overall solution to a laser spot tracker with a wide field of view.

In summary, the “best” diffuser depends on the performance requirements and constraints of each system on a case by case basis. As we saw in Section 4.4, the Spatial Transfer Function

can be a useful tool in evaluating overall performance. Additionally, there may not always be a diffuser with all of the ideal characteristics, in which case the diffuser selection becomes an optimization exercise. For example, a laser spot tracker with a very wide field of view whose tracking algorithm can deal with a circular Gaussian spot may benefit from using a Light Shaping Diffuser. Other systems with smaller FOVs may be able to deal with the aberration effects of an Engineered Diffuser. Some systems might benefit from the unique characteristics of a diffractive diffuser. Perhaps some systems could even use a simple lenslet array because the diffraction artifacts do not have enough of an impact on system performance. It should be clear that, by employing a detailed understanding of each diffuser, this thought process can be used when selecting a diffuser for any type of application. The only difference is the constraints that are placed on the selection process.

APPENDIX A: The Speckle Phenomenon

When a transmissive, rough object (i.e. one with surface feature sizes on the order of a wavelength) is illuminated by a monochromatic wave of light, such as a laser beam, it produces a grainy irradiance pattern in the transmitted field. This field can be thought of as a combination of an infinite number of wavelets, each corresponding to a different portion of the rough surface, as depicted in Figure A.1. The optical path length experienced by each wavelet differs slightly because of the height variations across the surface and this results in randomly distributed regions of constructive (bright) and destructive (dark) interference at the observation plane, producing the grainy appearance. This effect is known as speckle and an example is shown in Figure A.2. Note that this effect occurs in three dimensional space wherever the beamlets overlap.

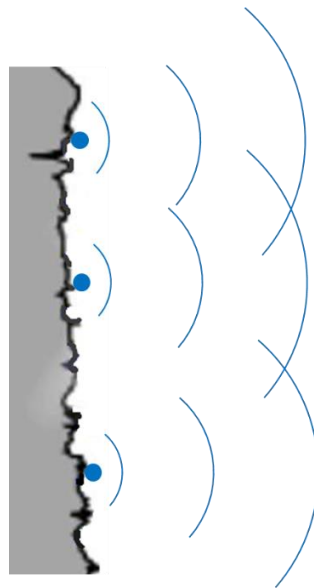


Figure A.1. Wavelets produced by a rough surface. All the wavelets interfere to produce a random speckle pattern.

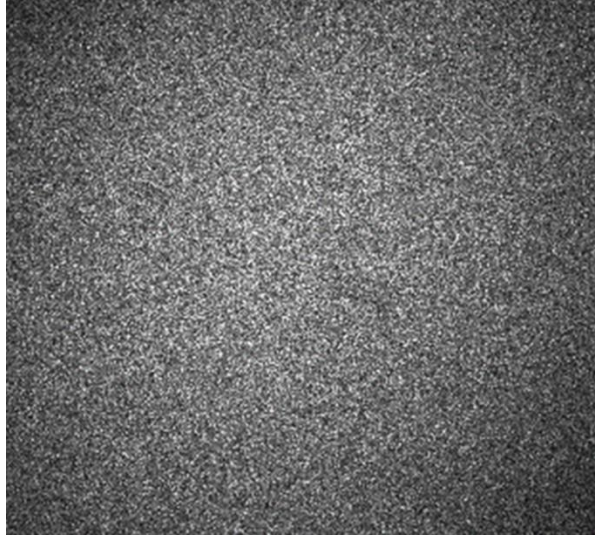


Figure A.2. Speckle pattern produced by a randomly rough surface illuminated by a laser.

When light from a beam of size D scatters from a diffuse surface and propagates through free space a distance L before reaching the observation plane, the size of the speckles σ' is approximately given by [1]

$$\sigma' \approx 1.2\lambda \frac{L}{D} . \quad (\text{Eq A.1})$$

This is known as objective speckle. Alternatively, if a lens is used to collect the scattered light and image it onto the observation plane the speckle pattern is known as subjective speckle. The size σ of the speckles formed this way depends on the focusing power (i.e. the numerical aperture) of the lens being used [1]:

$$\sigma \approx 0.6 \frac{\lambda}{NA} \approx 1.2(1 + M)\lambda F \quad (\text{Eq A.2})$$

where M is the magnification and F is the $F/\#$ of the imaging system. Manipulation of these parameters allows one to change the size and even the shape of the individual speckles [5]. For example, using a cylindrical lens will modify the NA in only one direction, causing the speckles to become elongated.

REFERENCES

- [1] Dainty, J.C, ed. Laser Speckle and Related Phenomena. 2nd ed. Vol. 9. New York: Springer-Verlag, 1984.
- [2] Kurtz et al. "Design and Synthesis of Random Phase Diffusers*." J. Opt. Soc. Am. 63.9 (1973): 1080.
- [3] "Diffuser Selection Guide." Edmundoptics.com. Web. 20 Nov. 2015.
- [4] Jansson et al. GRIN Type Diffuser Based On Volume Holographic Material. Physical Optics Corporation, assignee. Patent 5,365,354. 15 Nov. 1994.
- [5] Petersen et al. Homogenizer Formed Using Coherent Light and a Holographic Diffuser. Physical Optics Corporation, assignee. Patent 5,534,386. 9 Jul. 1996.
- [6] Milster, T. "Chapter 7: Miniature and Micro-Optics." Handbook of Optics. Ed. Michael Bass. Vol. 2. New York: McGraw-Hill, 2010.
- [7] Vasiljević et al. "Imaging Properties of Laser-produced Gaussian Profile Microlenses." Proc. of SPIE 6604 (2007).
- [8] Jenkins et al. Methods and Apparatus for Guidance Systems. Raytheon Company, assignee. Patent 7,530,528. 12 May 2009.
- [9] Layton, A. Binary Optics SAL Seeker (BOSS). Lockheed Martin Corporation, assignee. Patent 7,575,191. 18 Aug. 2009.
- [10] Pawluczyk, R. "Holographic Diffusers." Proc. of SPIE 2042 (1993).
- [11] Yeh, S. "A Study of Light Scattered by Surface-Relief Holographic Diffusers." Opt. Comm. 264 (2006) 1-8.
- [12] Goldenburg, J. and McKechnie, T. "Diffraction analysis of bulk diffusers for projection-screen applications." J. Opt. Soc. Am. A. 2.12 (1985): 2337.
- [13] Meyerhofer, D. "Holographic and Interferometric Viewing Screens." J. Appl. Opt. 12.9 (1973): 2180.
- [14] Salmanpour, A. and Nejad, S.M. "The Performance Improvement of the Target Position Determining System in Laser Tracking Based on 4Q Detector using Neural Network." World Academy of Science, Engineering and Technology 80 (2011): 548-51.

- [15] Miller, W. Electro-Optical De-Correlation of Wavefront Distortion Due to Atmospheric Scintillation. United States Army, assignee. Patent 3,562,537. 9 Feb. 1971.
- [16] Conrad, R. Wide Field-of-View Laser Spot Tracker. United States Army, assignee. Patent 4,574,191. 4 Mar. 1986.
- [17] Kress, B. C., and P. Meyrueis. "Chapter 4: Refractive Micro-Optics." Applied Digital Optics: From Micro-optics to Nanophotonics. Chichester, U.K.: Wiley, 2009.
- [18] Kress, B. C., and P. Meyrueis. "Chapter 6: Digital Diffractive Optics – Numeric Type." Applied Digital Optics: From Micro-optics to Nanophotonics. Chichester, U.K.: Wiley, 2009.
- [19] Kress, B. C., and P. Meyrueis. "Chapter 8: Digital Holographic Optics." Applied Digital Optics: From Micro-optics to Nanophotonics. Chichester, U.K.: Wiley, 2009.
- [20] Newport Website. www.newport.com.
- [21] Luminet, LLC Website. www.luminetco.com.
- [22] Thorlabs, Inc. Website. www.thorlabs.com.
- [23] RPC Photonics Website. www.rpcphotonics.com.
- [24] Lieberman et al. Monolithic Glass Light Shaping Diffuser and Method for its Production. Physical Optics Corporation, assignee. Patent 6,446,467. 10 Sep. 2002.
- [25] Coleman, C. Computer-Generated Holograms for Free-Space Optical Interconnects. Diss. U of Arizona, 1998.
- [26] Goodman, J. W. Introduction to Fourier Optics. 3rd ed. Greenwood Village: Roberts & Company, 2005.
- [27] Rantsch et al. Illuminating System. Zeiss, assignee. Patent 2,186,123. 21 Feb. 1938.
- [28] Donnelly, R. "The Simple Life." SPIE Newsroom, oemagazine, August (2004).
- [29] Ng, R. Digital Light Field Photography. Diss. Stanford Univ., 2006.
- [30] Hutley, M.C. "Chapter 5: Refractive Lenslet Arrays." Micro-optics Elements, Systems, and Applications. Ed. H.P Herzig. Bristol: Taylor & Francis, 1997.
- [31] Bright View Technologies Corporation Website. www.brightviewtechnologies.com.
- [32] BWF Offermann, Waldenfels & Co. Website. www.bwf-group.de/en/bwf-profiles.
- [33] iLumTech Website. www.ilumtech.eu.

- [34] LED Academy by OMS Lighting. "2. LED Optics." LEDacademy.net. 2015.
- [35] Méndez et al. "Design of One-dimensional Band-limited Uniform Diffusers of Light." *Appl. Phys. Lett.* 73.14 (1998): 1943-945.
- [36] Méndez et al. "The Design of Two-dimensional Random Surfaces with Specified Scattering Properties." *J. Opt. A: Pure Appl. Opt.* 7.2 (2005): S141-151.
- [37] Sales, T. Random Microlens Array for Optical Beam Shaping and Homogenization. Corning Inc., assignee. Patent 6,859,326. 22 Feb. 2005.
- [38] Morris et al. Structured Screens for Controlled Spreading of Light. Corning Inc., assignee. Patent 7,033,736. 25 Apr. 2006. Print.
- [39] Sales, T. "Structured Microlens Arrays for Beam Shaping." *Opt. Eng* 42.11 (2003): 3084-3085.
- [40] Sales, T. "Efficient and Uniform Illumination with Microlens-based Band-limited Diffusers." *Photonics Spectra* Apr. 2010
- [41] Glöckner, S., and R. Göring. "Investigation of Statistical Variations between Lenslets of Microlens Arrays." *Appl. Opt.* 36.19 (1997): 4438-445.
- [42] Sun et al. "Design and Evaluation of Blu-Ray Pickup Head System for Determining the Tilt Angle and Displacement of the Test Plane." *Opt. and Las. in Eng.* 49.8 (2011): 1076-1088.
- [43] Wolfe, W., and G. Zissis "The Infrared Handbook, Chapter 22: Tracking Systems," *Environmental Research Institute of Michigan*, Ann Arbor, MI, 1985.
- [44] Holo/Or Ltd. Website. www.holoor.com. "Optical Diffuser Application Notes."
- [45] http://fp.optics.arizona.edu/milster/optiscan/html/model_panel/introduction.html
- [46] Johnson et al. "Freeform Diffractive Structure Writing through Maskless Lithography," in *Frontiers in Optics 2014*, OSA (2014).